Synthetic and Structural Studies of Cobalt–Pivalate Complexes

Guillem Aromí,[a] Andrei S. Batsanov,[b] Paul Christian,[a] Madeleine Helliwell,[a] Andrew Parkin,[c] Simon Parsons,[c] Andrew A. Smith,[a] Grigore A. Timco,*[d] and Richard E. P. Winpenny*[a]

Abstract: The synthesis and characterisation of a range of cobalt pivalate cage complexes are reported. The cages include: a dinuclear Co^{II} complex; an oxo-centred Co^{III} triangle; tetranuclear Co^{II} heterocubanes and butterflies; tetranuclear heterovalent cobalt butterflies and hexanuclear edge-sharing bitetrahedra; heterovalent penta-, hexa- and hepta-nuclear cages based on $\{M_4O_4\}$ heterocubane cores; and a tetradecanuclear cage based on heterocubanes sharing edges and vertices. Spectroscopic studies suggest that some of these cores are retained in solution, but that only in the Co^{III} triangle is the structure including ligands retained. A scheme is proposed to account for the many structures observed, which may be applicable to other polymetallic cage complexes.

Keywords: cage compounds · carboxylate ligands · cobalt · self-assembly · structure elucidation · X-ray diffraction

Introduction

One of the great challenges in polynuclear coordination chemistry is to establish reliable synthetic routes to oligomeric structures. Frequently complexes form that appear as isolated examples of a structural motif, and where there seems no relationship between the polynuclear cage and the substrate used to synthesise this cage. In this paper we report our systematic exploration of the coordination chemistry of cobalt pivalate cages. Previously we have reported on chromium pivalates—whereby a dodecanuclear Cr^{III} cage,[1] an octanuclear Cr^{III} wheel[2] and several smaller Cr triangles[3] could be isolated. We have also reported the reactions of cobalt(II) and nickel(II) with pivalate in the presence of pyridonate ligands.[4] Here we discuss the many small clusters—dinuclear to tetradecanuclear—that can be simply prepared which involve cobalt and the pivalate ligand. Eremenko and co-workers have also been investigating cobalt and nickel pivalate chemistry.[5]

Results

Synthesis and structures: The seemingly simple system involving cobalt and pivalate is extremely rich, and very minor changes in reaction conditions and crystallisation solvents lead to a range of polynuclear cages. These results are summarised in Scheme 1. Analytical data are given in Table 1.

The starting point for much of this chemistry are the dinuclear complexes $[Co_2(\mu\text{-}OH_2)(O_2CCMe_3)_4(HO_2CCMe_3)_4]$ (**1**; Figure 1) and $[Co_2(\mu\text{-}OH_2)(O_2CCMe_3)_4(HO_2CCMe_3)_2(py)_2]$ (**2**; Figure 2). Complex **1** is made by direct reaction of cobalt carbonate with pivalic acid, followed by crystallisation from MeCN, while **2** is made by the addition of pyridine to a solution of **1** in pivalic acid and CH_3CN.

The cores of both **1** and **2** are very similar. In both, the two cobalt(II) sites are bridged by two 2.11-carboxylates (Harris notation[6]) and by an oxygen atom, which we assign as a μ-water molecule. In **1** the coordination spheres at each six-coordinate Co site is completed by two protonated pivalate ligands, and by one deprotonated pivalate; in **2** one of the protonated pivalates is replaced by pyridine at each cobalt. A similar compound, $[Co_2(\mu\text{-}OH_2)(O_2CCMe_3)_4(py)_4]$, in which all terminal ligands are pyridine has been reported by

---

[a] Prof. R. E. P. Winpenny, Dr. G. Aromí, Dr. P. Christian,
Dr. M. Helliwell, Dr. A. A. Smith
Department of Chemistry, The University of Manchester
Oxford Road, Manchester, M13 9PL (UK)
Fax: (+44) 161-275-4616
E-mail: richard.winpenny@man.ac.uk

[b] Dr. A. S. Batsanov
Department of Chemistry, The University of Durham
South Road, Durham, DH1 3LE (UK)

[c] Dr. A. Parkin, Dr. S. Parsons
Department of Chemistry, The University of Edinburgh
West Mains Road, Edinburgh, EH9 3JJ (UK)

[d] Dr. G. A. Timco
Institute of Chemistry, Moldova Academy of Sciences
Academy Str. 3, Chisinau 2028 (Republic of Moldova)
Fax: (+373) 72-97-61
E-mail: timg@nor.md

DOI: 10.1002/chem.200304993

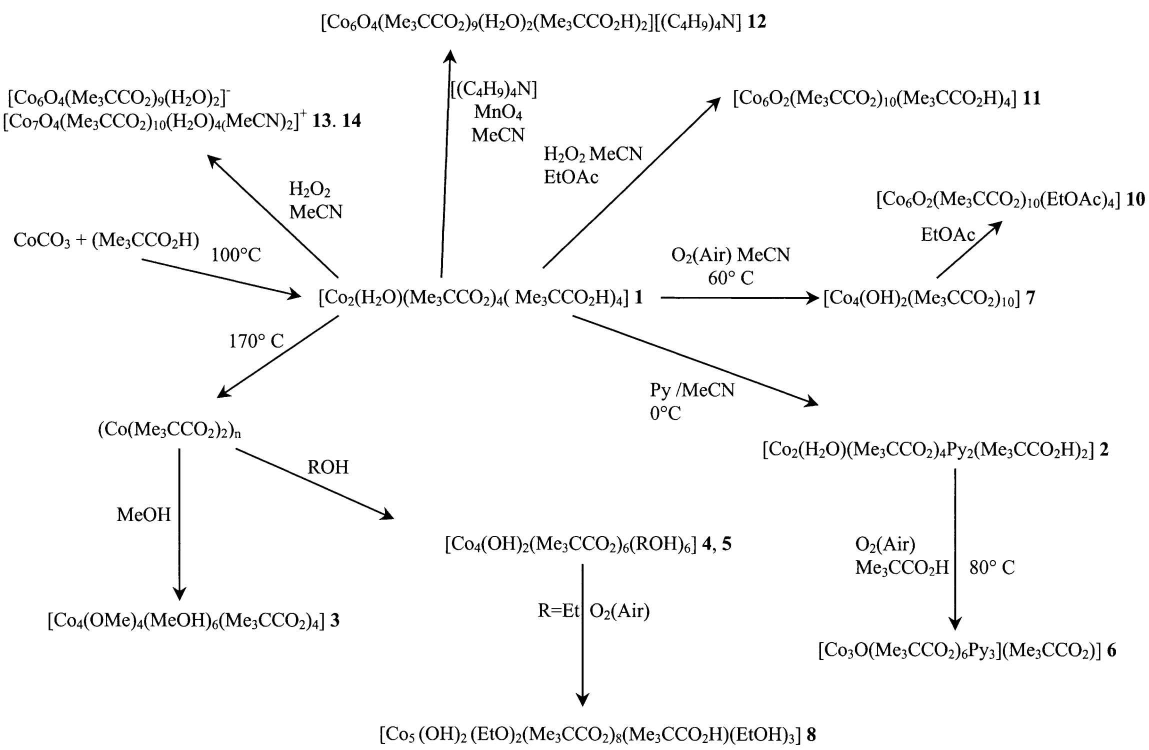

Scheme 1.

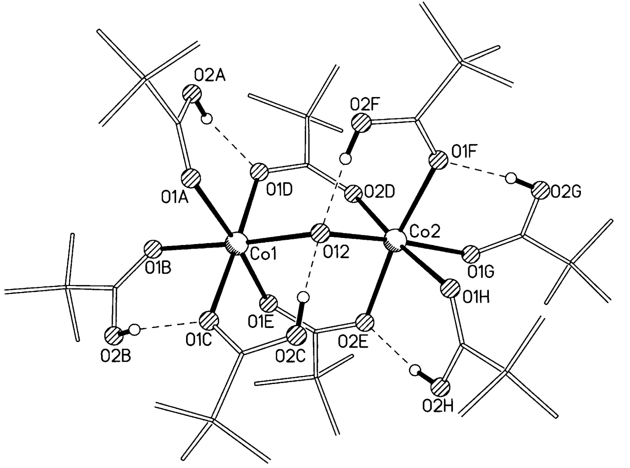

Figure 1. The structure of $[Co_2(\mu\text{-}OH_2)(O_2CCMe_3)_4(HO_2CCMe_3)_4]$ (**1**) in the crystal.

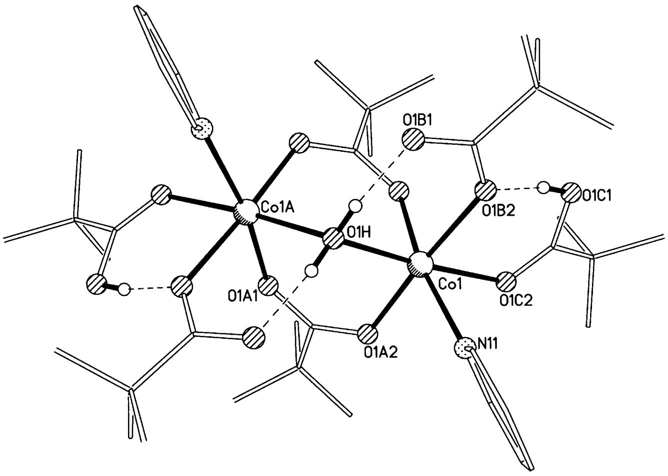

Figure 2. The structure of $[Co_2(\mu\text{-}OH_2)(O_2CCMe_3)_4(HO_2CCMe_3)_2(py)_2]$ (**2**) in the crystal.

Table 1. Analytical data[a] for compounds **1** to **15**.

		C	H	N	Co
1	$[Co_2(\mu\text{-}OH_2)(O_2CCMe_3)_4(HO_2CCMe_3)_4]$	50.6(50.6)	8.3(8.3)	0.0(0.0)	11.9(12.4)
2	$[Co_2(\mu\text{-}OH_2)(O_2CCMe_3)_4(HO_2CCMe_3)_2(py)_2]$	53.1(53.2)	7.7(7.6)	3.2(3.1)	13.1(13.1)
A	$[Co(O_2CCMe_3)_2]_n$	45.7(46.0)	6.9(7.0)	0.0(0.0)	22.5(22.6)
3	$[Co_4(\mu_3\text{-}OMe)_4(O_2CCMe_3)_4(MeOH)_4]\cdot 4.5\,MeOH$	37.5(37.7)	6.7(7.2)	0.0(0.0)	26.8(26.4)
4	$[Co_4(\mu_3\text{-}OH)_2(O_2CCMe_3)_6(EtOH)_6]\cdot 2\,EtOH$	43.8(44.4)	8.2(8.4)	0.0(0.0)	18.7(18.9)
5	$[Co_4(\mu_3\text{-}OH)_2(O_2CCMe_3)_6(n\text{PrOH})_6]\cdot 2\,PrOH$	46.8(46.6)	8.8(8.5)	0.0(0.0)	18.8(19.1)
6	$[Co_3(\mu_3\text{-}O)(O_2CCMe_3)_6(py)_3]_2.(O_2CCMe_3)_2\cdot 7\,HO_2CCMe_3\cdot 2\,H_2O$	54.0(53.6)	7.8(7.7)	2.7(2.8)	11.6(11.7)
8	$[Co_5(\mu_3\text{-}OH)_2(\mu\text{-}OEt)_2(O_2CCMe_3)_8(HO_2CCMe_3)(EtOH)_3]\cdot HO_2CCMe_3$	45.8(45.9)	8.0(7.8)	0.0(0.0)	18.4(18.8)
9	$[Co_5(\mu_3\text{-}OH)_2(\mu\text{-}OEt)_2(O_2CCMe_3)_8(EtOH)_4]\cdot 2\,EtOH$	44.2(44.7)	7.5(8.0)	0.0(0.0)	20.0(19.6)
10	$[Co_6(\mu_4\text{-}O)_2(O_2CCMe_3)_{10}(EtOAc)_2]\cdot 0.5\,EtOAc$	45.5(44.6)	7.2(6.9)	0.0(0.0)	21.0(21.9)
11	$[Co_6(\mu_4\text{-}O)_2(O_2CCMe_3)_{10}(HO_2CCMe_3)_4]\cdot 0.25\,EtOAc$	47.2(46.9)	7.4(7.4)	0.0(0.0)	18.6(18.7)
12	$[(C_4H_9)_4N][Co_6O_4(O_2CCMe_3)_9(H_2O)_2(HO_2CCMe_3H)_2]\cdot 2\,MeNO_2$	44.6(45.4)	7.8(7.7)	2.0(2.2)	16.6(18.3)
13·14	$[Co_7(\mu_4\text{-}O)_3(\mu_3\text{-}O)(O_2CCMe_3)_9(HO_2CCMe_3)(H_2O)_3(MeCN)_2]$ $[Co_6(\mu_4\text{-}O)_2(\mu_3\text{-}O)_2(O_2CCMe_3)_9(H_2O)_2]\cdot 3\,Me_3CCO_2H\cdot 2\,H_2O$	41.0(41.1)	6.7(6.7)	0.7(0.8)	22.7(23.0)
15	$[Co_{14}(\mu_5\text{-}O)_2(\mu_3\text{-}O)_2(\mu_3\text{-}OH)_{12}(O_2CCMe_3)_{14}(HO_2CCMe_3)_2\,(H_2O)_6(MeCN)_2]$	36.3(34.8)	6.5(6.1)	0.0(1.0)	[b]
16	$[Co_{14}O_4(OH)_{12}(O_2CCMe_3)_{14}(H_2O)_8(HO_2CCMe_3)_3]$	35.0(34.5)	6.5(6.2)	0.0(0.0)	[b]

[a] Calculated values are given in parentheses. [b] Not measured.

Eremenko et al.[5] The deprotonated pivalates form strong hydrogen bonds (2.55 Å in **1** and 2.62 Å in **2**) to the μ-OH_2. This raises a question of whether the more accurate description is as a μ-OH_2 and two deprotonated pivalates or as a μ-O and two HO_2CCMe_3 ligands. Valence-bond sum analysis—with a method developed by Brown[7a]—supports the presence of Co^{II} (Table 2). The Co–O bonds then lie between those expected for Co^{II}–(OH) (average 1.91 Å) and Co^{II}–(H_2O) (average 2.14 Å);[7] this is consistent with the strong hydrogen bonding found. Further hydrogen bonds are found between terminal HO_2CCMe_3 ligands and deprotonated O atoms of pivalates. The O···O contacts for these bonds vary from 2.55 to 2.59 Å.

Table 2. Bond valence sum analysis for cobalt sites in **1**–**15**.

Complex	Co center	BVS[a]	Co center	BVS[a]	Assigned O.S.
1	1	2.030	2	2.027	2
2	1	2.298	2	2.298	2
3	1	1.963	2	1.946	2
	3	1.991	4	2.005	2
4[b]	1	2.130	2	2.173	2
5	1	2.036	2	1.940	2
	3	1.940	4	1.993	2
6	1	2.880	2	2.996	3
	3	2.991			3
7	1	3.069	2	3.028	3
	3	2.828	4	2.978	3
8	1	2.054	3	1.930	2
	2	2.907	4	2.904	3
	5	2.042			2
9	1	2.039	3	1.905	2
	2	2.899	4	2.878	3
	5	2.041			2
10[c]	1	1.979	2	1.848	2
	3	2.871			3
11	1	1.987	2	1.959	2
	3	2.770	4	2.828	3
	5	1.961	6	1.951	2
12	1	2.889	2	2.944	3
	3	2.930	4	2.944	3
	5	1.961	6	1.951	2
13	1	1.989	3	1.989	2
	2	3.001	4	2.982	3
	5	2.984	6	2.953	3
14	1	1.906	2	1.909	2
	3	1.900			2
	4	2.938	5	2.961	3
	6	2.896	7	2.960	3
15	1	2.948	2	2.841	3
	3	2.890	4	3.136	3
	5	1.995	6	2.011	2
	7	1.969			2

[a] Values used for calculation of sum obtained from Cambridge Structure Database using the method of I. D. Brown. Values for r_o pertain to those obtained from transition metal complexes.[7] [b] There are two cobalt sites in the asymmetric unit. [c] There are three cobalt sites in the asymmetric unit.

Two types of reactions starting with these dimers have been investigated. The first is oligomerisation by means of thermal decomposition followed by crystallisation from alcohols, while the second is oxidation—either of the dinuclear complexes or of the alcohol complexes.

Heating **1** to 180 °C leads to an ill-defined compound that analyses well for "$Co(O_2CCMe_3)_2$" (**A**). This formula is also supported by thermogravimetric analysis of **1**. Other routes to this compound have been reported.[8, 9] We believe this compound is probably polymeric as it has unusually low solubility in nonpolar solvents for complexes of pivalate. Complex **A** is extremely reactive, dissolving and reacting with a range of alcohols. In MeOH a tetranuclear heterocubane, $[Co_4(\mu_3\text{-}OMe)_4(O_2CCMe_3)_4(MeOH)_4]$ (**3**), forms with methoxide supplying the O atoms at the alternate sites of the heterocubane (Figure 3). Two 1.11-pivalates chelate to each of Co1 and Co2. Two further pivalates act as 2.11-bridges between Co1 and Co2, and Co3 and Co4, respectively. The remaining coordination sites on Co3 and Co4 are occupied by four MeOH ligands.

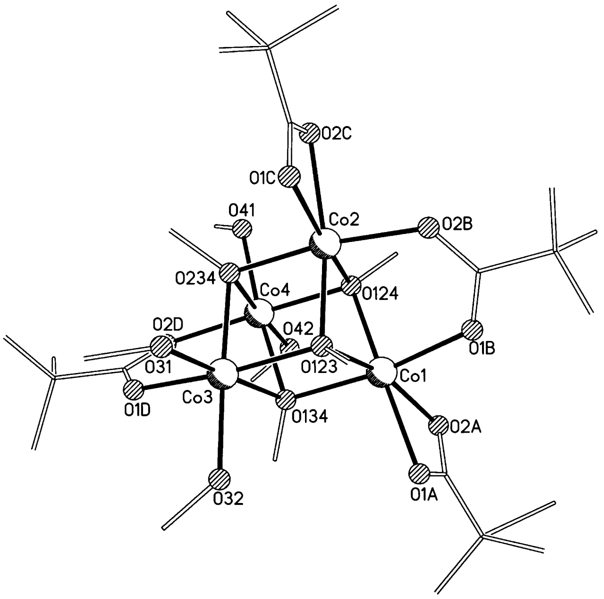

Figure 3. The structure of $[Co_4(\mu_3\text{-}OMe)_4(O_2CCMe_3)_4(MeOH)_4]$ (**3**) in the crystal.

There are two distinct cobalt sites in **3**. Two involve chelating pivalates, while two are each bound to two terminal solvates. The reaction of **A** with other alcohols also produces tetranuclear cages in which there are two distinct cobalt sites (Figure 4). However, in EtOH and *n*PrOH the differences between the sites are more pronounced than in **3**. $[Co_4(\mu_3\text{-}OH)_2(O_2CCMe_3)_6(ROH)_6]$ (R = Et, **4**; R = *n*Pr, **5**) contains a rhombus of cobalt(II) sites, with the short diagonal of the rhombus (Co2 and Co2a) bridged by two μ3-hydroxides; these OH groups also bridge to Co sites at the end of the long diagonal (Co1 and Co1a). Two of the edges of the rhombus are also bridged by two 2.11-pivalates, while the two alternating edges have no bridge beyond the μ3-OH. All the metal sites are six-coordinate, with the coordination sphere at the wing-tip sites completed by a chelating pivalate and one ROH molecule, while at the body sites the coordination is completed by two ROH molecules. The structures of **4** and **5** can be regarded as a dimerisation of **1** and **2**, with the "dinuclear" fragment comprising one body and one wing-tip cobalt bridged by a μ-OH and two pivalates that has dimerised through the hydroxide group binding to a second dinuclear block.

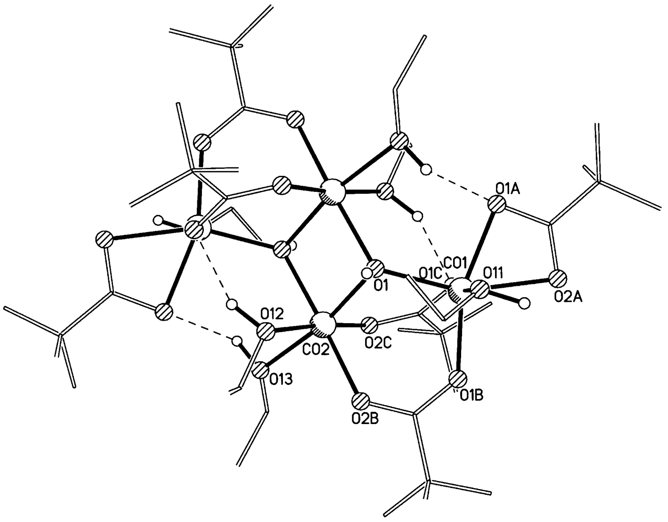

Figure 4. The structure of $[Co_4(\mu_3\text{-}OH)_2(O_2CCMe_3)_6(EtOH)_6]$ (**4**) in the crystal.

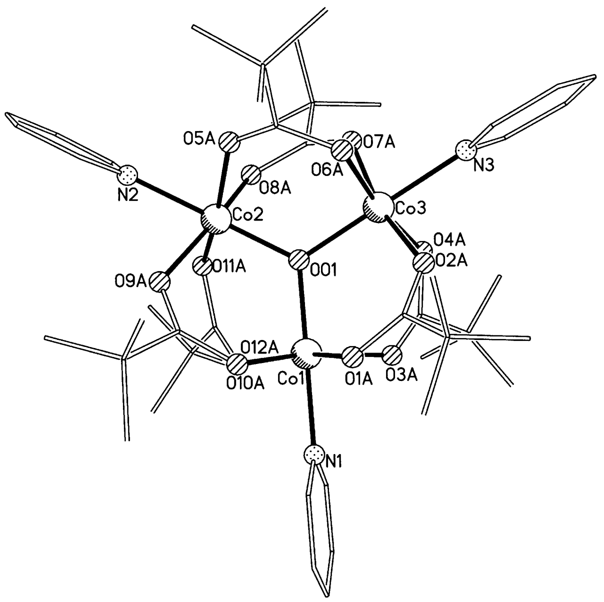

Figure 5. The structure of $[Co_3(\mu_3\text{-}O)(O_2CCMe_3)_6(py)_3]$ (**6**) in the crystal.

The difference in reactivity that leads to **3**, **4** and **5** is presumably related to the ease of deprotonation of MeOH, EtOH and *n*PrOH. While methoxide is found in **3**, no alkoxides are found in **4** or **5**. Therefore the more protic solvent leads to a heterocubane, while the less acidic solvent retains the proton and merely coordinates in vacant sites on the periphery of the cage. Valence bond sum (VBS) analysis shows in all three cages that cobalt(II) is present (Table 2).

The second reaction type investigated is oxidation of the di- and tetranuclear cages. Complex **1** in pyridine/pivalic acid mixture or complex **2** in pivalic acid can be readily oxidised by air to a trinuclear cage $[Co_3(\mu_3\text{-}O)(O_2CCMe_3)_6(py)_3]^+$ (**6**), while **1** is oxidised by air in $MeCN/HO_2CCMe_3$ to give a tetranuclear cage $[Co_4(\mu_3\text{-}OH)_2(O_2CCMe_3)_9(HO_2CCMe_3)]$ (**7**); the structures of these two cages are closely related. The crystals of **7** were taken directly from the reaction solution without recrystallisation. Complex **7** is probably an intermediate and the final product of this reaction (product **B**) probably has a higher nuclearity. Complex **7** cannot be isolated in a pure form, and recrystallisation of **B** leads to penta- or hexanuclear cages depending on the solvent used (see below).

Complex **6** is a typical oxo-centred carboxylate triangle, featuring exclusively Co^{III} sites around a central μ_3-oxide (Figure 5). Each edge of the triangle is further bridged by two 2.11-pivalates, with a terminal pyridine ligand completing the coordination environment around each octahedral cobalt site. A similar oxo-centred cobalt(III) triangle has been reported for acetate.[10] VBS is in good agreement with the assignment of oxidation state. There is a very large amount of co-crystallised pivalate and pivalic acid in the lattice. The hydrogen bonding between these species is discussed below.

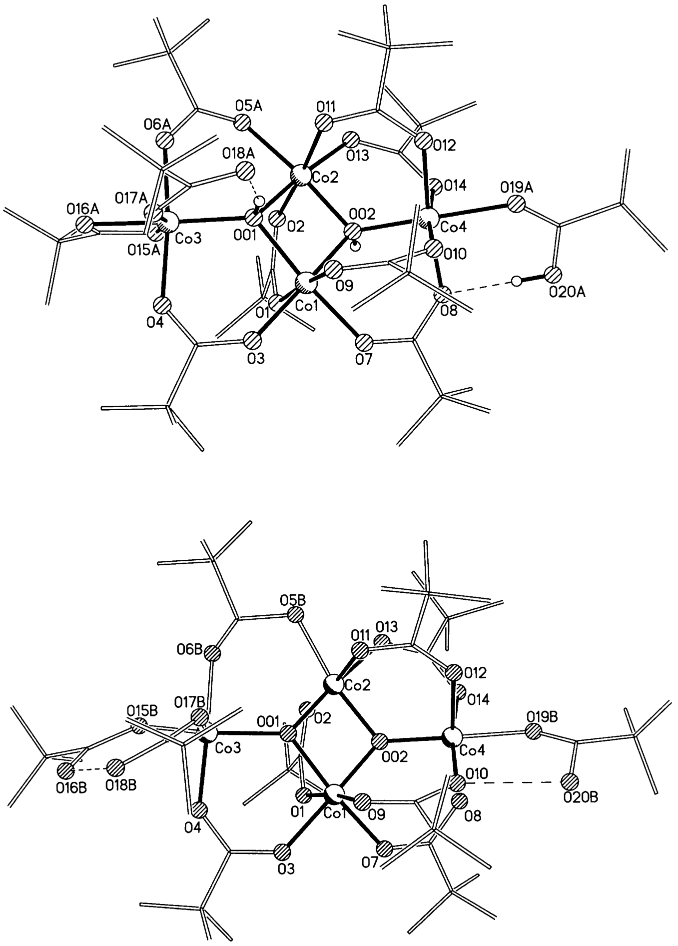

Figure 6. Top: The structure of the major component of $[Co_4(\mu_3\text{-}OH)_2(O_2CCMe_3)_9(HO_2CCMe_3)]$ (**7**) in the crystal. Bottom: the structure of the minor component of **7** in the crystal.

Complex **7** appears to be mixed-valent; however, disorder in the ligands creates some confusion about the exact oxidation state. In the major component of the crystal (Figure 6, top) all the cobalt sites are six-coordinate, and there are seven 1,3-bridging pivalates, one chelating pivalate and two pivalates involved in the hydrogen bonding. One of these latter pivalates is a hydrogen-bond donor through O20A ($O\cdots O$ distance 2.58 Å), while the second is a hydrogen-bond acceptor through O18A which is interacting with a bridging hydroxide (O01) (O⋯O distance 2.45 Å). As the second O atom of this pivalate is bound to Co3, this pivalate must also be deprotonated, and, therefore, the formula of the major component of the crystal is $[Co_4(\mu_3\text{-}OH)_2(O_2CCMe_3)_9(HO_2CCMe_3)]$. This would require one Co^{II} and three Co^{III} sites for charge balance.

In the minor component of the crystal (Figure 6, bottom) the chelating pivalate has been displaced and is involved in a hydrogen-bonding interaction. The bond is shown between O16B and O18B. The atom O18B is from the pivalate that was hydrogen bonding to the bridging hydroxide in the major component. One of these two pivalates must, therefore, now be protonated in the minor component, and the formula is $[Co_4(\mu_3\text{-}OH)_2(O_2CCMe_3)_8(HO_2CCMe_3)_2]$. This is requires two Co^{II} and two Co^{III} centres for charge neutrality. One cobalt site (Co3) is five-coordinate, with a square pyramidal geometry. The ratio of major to minor components is approximately 3:1 in the crystal lattice.

The structure of **7** consists of a rhombus of four cobalt atoms, containing two μ-OH groups. The way the edges of the rhombus are bridged makes the structure quite distinct from **4** and **5**. Two edges (Co1⋯Co4 and Co2⋯Co4) are bridged by two 1,3-pivalates in a similar manner to the edges of the oxo-centred triangle **6**. The third edge of this "triangle" (Co1⋯Co2) is bridged by a single pivalate and the central hydroxide of the second triangle of the rhombus (O01). The other edges of the second triangle (Co2⋯Co3 and Co1⋯Co3) are each bridged by a single carboxylate. The cobalt atoms on the short diagonal of the rhombus are, therefore, bound exclusively to bridging groups—two hydroxides and four pivalate oxygens. The Co4 atom at one periphery is bound to four bridging pivalates, one OH and a terminal protonated pivalate (O19); there is a minor disorder in this ligand, which has two orientations but similar hydrogen bonding in each.

VBS analysis supports all sites being Co^{III} with no significant difference to the metal sites in **6**. This is a failure for VBS, and may be due to the disorder in the structure. While the oxidation state could fit if the bridging hydroxides were reassigned as oxide, this does not match the clearly pyramidal bond angles about the O atoms concerned, that is, the sum of the three Co-O-Co angles is not close to 360°.

Aerial oxidation of the solution from which crystals of the tetranuclear cage **4** grew leads to a further complex: $[Co_5(\mu_3\text{-}OH)_2(\mu\text{-}OEt)(\mu_3\text{-}OEt)(O_2CCMe_3)_8(HO_2CCMe_3)\ (EtOH)_3]$ (**8**; Figure 7). The nuclearity and structure are unexpected. Complex **8** can be described based on a tetranuclear rhomboid core, as in **4**, **5** and **7**, but a more natural description is as an incomplete bicapped heterocubane. The heterocubane contains three cobalt sites (Co2, Co3 and Co4) and two μ_3-hydroxides (O10 and O13) and two μ-ethoxide oxygen atoms (O11 and O12). The hydroxides each bridge to one of the capping cobalt atoms (Co1 and Co5). Complex **4** can easily be related to the dimer **1** from which it was made; the same is true of **8**. Here the "building blocks" Co1⋯Co2 and Co4⋯Co5 are each bridged by two pivalates and a hydroxide, but now the two hydroxides, rather than bridging to the second dimer (as in **4**) attach to an additional cobalt site (Co3). In addition to these edges which are doubly bridged by pivalates, single pivalates bridge the edges Co1⋯Co3, Co3⋯Co5 and Co2⋯Co4. Each cobalt site is six-coordinate; charge balance requires two Co^{III} and three Co^{II} ions. VBS analysis shows that Co1, Co3 and Co5 are Co^{II} sites, with the remaining sites Co^{III}.

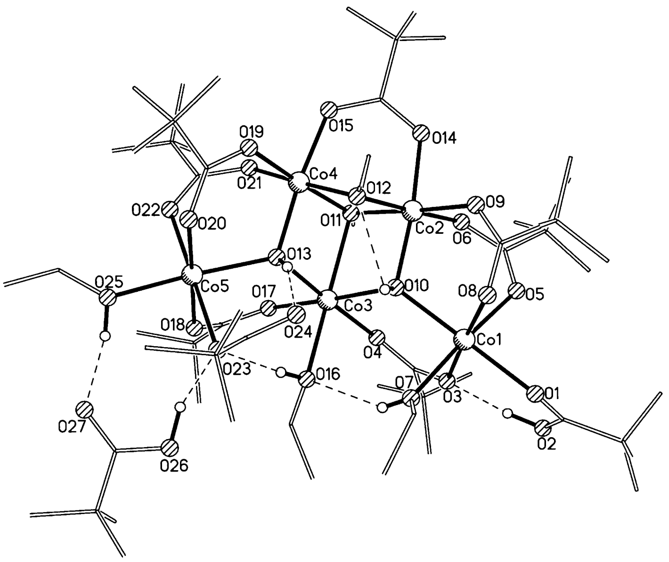

Figure 7. The structure of $[Co_5(\mu_3\text{-}OH)_2(\mu\text{-}OEt)_2(O_2CCMe_3)_8(HO_2CCMe_3)(EtOH)_3]$ (**8**) in the crystal.

There is significant hydrogen bonding in **8**. One bridging hydroxide interacts with the μ-OEt group (O⋯O distance 2.57 Å), while the second hydrogen bonds to a pivalate oxygen (O⋯O distance 2.77 Å). A terminal pivalic acid group (O2) donates a proton to a hydrogen bond to O3, part of a pivalic acid (O⋯O distance 2.60 Å). There is a hydrogen bond from one terminal EtOH (O7) to the other (O16) (O⋯O distance 2.84 Å), while the second also hydrogen bonds to a pivalate oxygen (O23) (O⋯O distance 2.77 Å). Finally, two hydrogen bonds attach a pivalic acid molecule to the cage (O25⋯O27 2.71 Å, O23⋯O26 2.58 Å).

Complex **8** is a minor product isolated from slow oxidation of the solution which gave the cobalt(II) rhombus **4**. However if **B**, the product of oxidation of **1** by air in MeCN/HO_2CCMe_3, is dissolved in EtOH and the solution left for one day at room temperature before cooling to −30 °C, after approximately one week green crystals of $[Co_5(\mu_3\text{-}OH)_2(\mu\text{-}OEt)_2(O_2CCMe_3)_8(EtOH)_4]\cdot 2\,EtOH$ (**9**) grow. This solution also contains a small number of pink crystals that, from a unit cell determination, are **4**. The best synthesis of **9** is from dissolution of a hexanuclear cage, $[Co_6(\mu_4\text{-}O)_2(O_2CCMe_3)_{10}(EtOAc)_2]$ (**10**), in EtOH; this avoids co-crystallisation of **4**. Complex **9** contains the same incomplete bicapped cubane core as **8**, but with one terminal pivalic acid ligand (attached to Co5 in **8**) replaced by a terminal EtOH (attached to Co1 in **9**). The metal sites are again a mixture of Co^{II} (Co1, Co3 and Co5) and Co^{III} (Co2 and Co4).

As in **8** there is a large amount of hydrogen bonding. The bridging hydroxides hydrogen bond to the bridging ethoxides (O⋯O distances 2.57 to 2.61 Å); an oddity is that there is no difference between the distance to the μ_3-OEt and to the μ-OEt. There are two pivalate–EtOH hydrogen bonds (O⋯O distances 2.69 and 2.80 Å), and three hydrogen bonds link three EtOH molecules (O⋯O distances 2.687 to 2.89 Å). A further EtOH molecule is only attached to the cage through hydrogen bonds, and also binds to a terminal pivalate group in a neighbouring cage. The hydrogen bonding in **9** therefore provides weak intermolecular interactions.

If **B** is recrystallised from EtOAc, crystals of **10** grow. $[Co_6(\mu_4\text{-}O)_2(O_2CCMe_3)_{10}(EtOAc)_2]$ (**10**) contains an edge-sharing bitetrahedron of cobalt sites (Figure 8). The molecule lies on a crystallographic twofold axis. Charge balance requires two Co^{III} and four Co^{II} sites. VBS shows that of the three unique Co sites, Co3 is clearly Co^{III} and Co1 and Co2 are Co^{II} centres. Co1 and Co3 have octahedral coordination spheres, while Co2 is tetrahedral. The coordination sphere of each centre consists of one of the μ_4-oxides, with the remainder consisting of pivalate O atoms, with the exception of one site of Co1 where an EtOAc molecule is found. Each of the ten external edges of the bitetrahedron is bridged by a single pivalate, for example, Co2···Co3 is bridged by the pivalate containing O8 and O9. If **10** is redissolved in EtOH and the solution cooled to −30 °C crystals of **9** form.

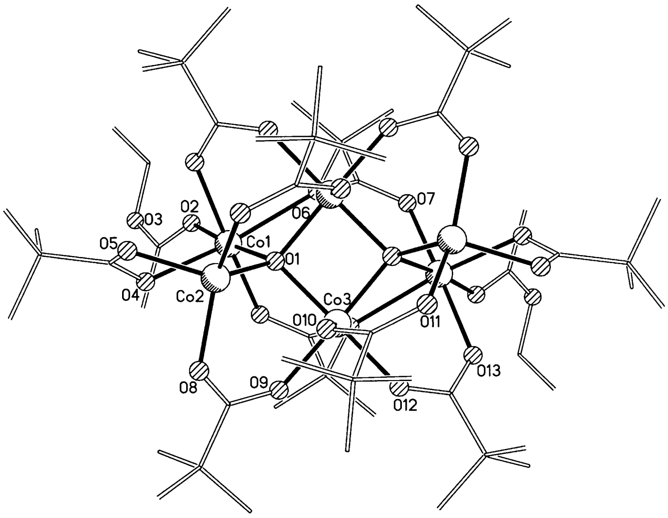

Figure 8. The structure of $[Co_6(\mu_4\text{-}O)_2(O_2CCMe_3)_{10}(EtOAc)_2]$ (**10**) in the crystal.

If an excess of peroxide is added we can generate further pivalate cages. Use of 0.68 wt % of hydrogen peroxide, followed by crystallisation from EtOAc generates a further edge-sharing bitetrahedron $[Co_6(\mu_4\text{-}O)_2(O_2CCMe_3)_{10}(HO_2CCMe_3)_4]$ (**11**; Figure 9). The oxidation states are again two Co^{III} and four Co^{II} sites. VBS shows clearly that Co3 and Co4 are in the higher oxidation state with the other sites Co^{II}; as in **10** it is the two cobalt centres in the shared edge that have the higher oxidation state. In **11** all cobalt sites are six-coordinate. The bridging motifs are very similar to **10**, that is, two μ_4-oxides and each edge of the polyhedron bridged by a single pivalate; however, two pivalates have become 3.21-bridging, for example, O2C is μ_2-bridging between Co4 and Co5. The other change from **10** is that the two terminal EtOAc molecules have been displaced, and four terminal pivalic acid molecules are found—one attached to each of the external vertices of the bitetrahedron.

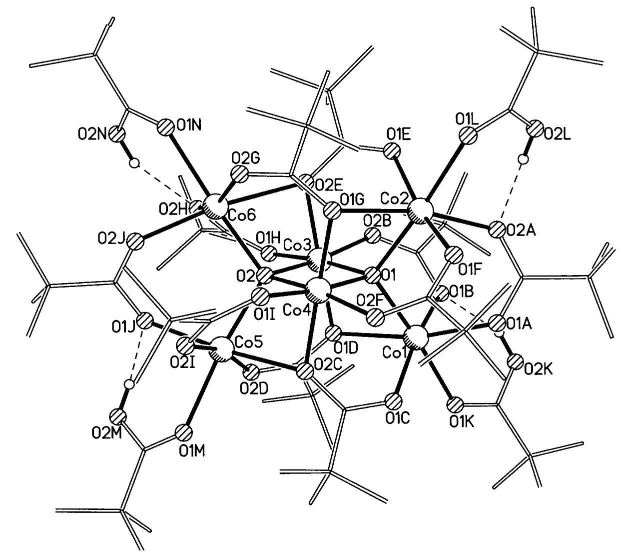

Figure 9. The structure of $[Co_6(\mu_4\text{-}O)_2(O_2CCMe_3)_{10}(HO_2CCMe_3)_4]$ (**11**) in the crystal.

While there is no significant hydrogen bonding in **10**, in **11** there are four hydrogen bonds between terminal pivalic acid groups and bridging pivalates (O···O distances 2.55 to 2.67 Å).

Performing the oxidation using $[(C_4H_9)_4N][MnO_4]$ in MeCN leads to a very dark green gel from which crystals of $[(C_4H_9)_4N][Co_6O_4(O_2CCMe_3)_9(H_2O)_2]$ (**12**) can be grown (Figure 10). There is some disorder in the cation, but there is no doubt the hexanuclear cage is a monoanion. Complex **12** contains a central $\{Co_4O_4\}$ heterocubane in which all the cobalt sites are Co^{III}. Two of the oxides are μ_3-bridging—binding only to Co centres within the heterocubane—while two are μ_4-bridging—attaching two further cobalt atoms to the core. These additional Co sites are clearly Co^{II}. One of the Co^{II} sites (Co5) is five coordinate, while the second (Co6) is four-coordinate; the difference is the presence of a bridging pivalate (O14) attached to Co5. All the Co^{III} sites are six

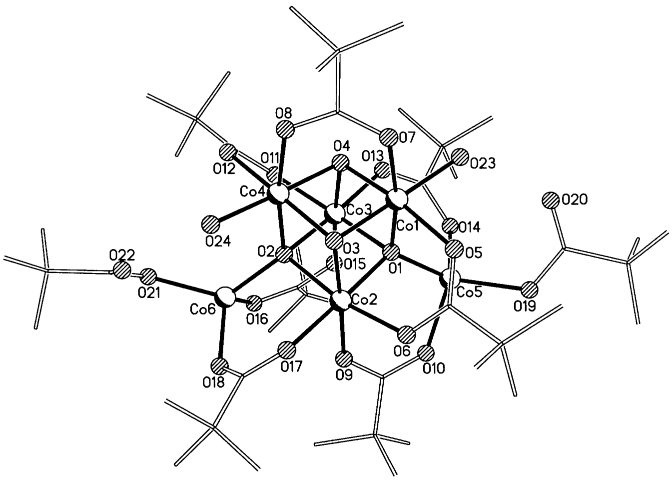

Figure 10. The structure of $[(C_4H_9)_4N][Co_6O_4(O_2CCMe_3)_9(H_2O)_2]$ (**12**) in the crystal.

coordinate. Terminal water ligands are attached to Co1 and Co2, which are also bound to three bridging oxides and two O atoms from pivalate; Co2 and Co3 are bound to three oxides and three pivalate oxygens. Pivalates bridge three faces of the cubane: Co1 ··· Co2, Co1 ··· Co4 and Co3 ··· Co4. Two pivalates bridged from each of the "capping" Co^{II} sites to the cubane.

Hydrogen bonding is again significant in the structure. Two additional pivalic acid molecules are attached to the cage, in each case through hydrogen-bond donation to a μ_3-oxide and accepting a proton from a terminal water. The two terminal water molecules also find additional contacts, for example, O21 ··· O24 = 2.62 Å.

With stronger hydrogen peroxide (30 wt %) a brown solid is produced which dissolves in MeCN, and which crystallises to give a pair of clusters $[Co_7(\mu_4\text{-}O)_3(\mu_3\text{-}O)(O_2CCMe_3)_9(HO_2CCMe_3)(H_2O)_3(MeCN)_2][Co_6(\mu_4\text{-}O)_2(\mu_3\text{-}O)_2(O_2CCMe_3)_9(H_2O)_2]$ (**13**·**14**). We assume the $\{Co_7\}$ cage **13** is the cation and the $\{Co_6\}$ cage **14** is the anion. Both are mixed-valent, and are closely related.

Anion **14** has a very similar structure to **12**, containing a similar central $\{Co^{III}_4O_4\}$ heterocubane, in which two of the oxides bind to Co centres within the heterocubane, while two attach two Co^{II} sites to the core. In **14** these Co^{II} sites are four-coordinate. Assignment of oxidation state is supported by VBS analysis, and makes **14** a monoanion. Hydrogen bonding is fairly restricted, with a single hydrogen bond to each of the terminal water molecules from a pivalate.

In **13** a similar $\{Co_4O_4\}$ heterocubane is found, but now caps are found on three of the O atoms (Figure 11). Again it is clear from VBS analysis (Table 2) that the four cobalt sites of the cubane are Co^{III} and the three caps are Co^{II}. The caps are five-coordinate, while the cubane sites are six-coordinate. As in **12** three pivalates bridge faces of the cubane (Co9 ··· Co10, Co10 ··· Co8 and Co8 ··· Co9) and two bridge from the cubane to each of the capping Co sites, for example, bridges are present from Co8 to Co12 and Co7 to Co12. The caps are each bound to one μ_4-oxide, two pivalate oxygens and one O atom from a water molecule, with Co11 and Co13 each additionally bound to a single MeCN molecule and Co12 bound to a molecule of pivalic acid. The only hydrogen bond in the structure also involves this pivalic acid, and is to a bridging pivalate (O ··· O distance 2.64 Å)

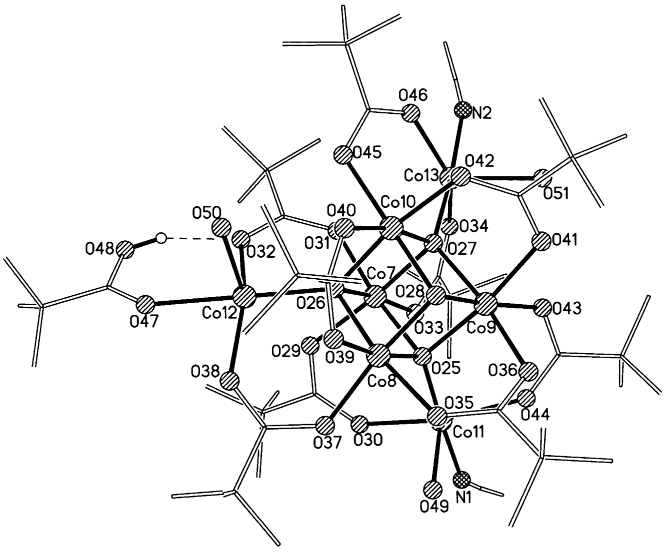

Figure 11. The structure of $[Co_7(\mu_4\text{-}O)_3(\mu_3\text{-}O)(O_2CCMe_3)_9(HO_2CCMe_3)(H_2O)_3(MeCN)_2]$ (**13**) in the crystal.

The importance of the oxidant used led us to investigate to further oxidising agents. Reaction of **1** with either *tert*-butylperoxide or with potassium dichromate led to new tetradecanuclear cages: $[Co_{14}O_4(OH)_{12}(O_2CCMe_3)_{14}(HO_2CCMe_3)_2(H_2O)_6(MeCN)_2]$ (**15**) and $[Co_{14}O_4(OH)_{12}(O_2CCMe_3)_{14}(H_2O)_8(HO_2CCMe_3)_3]$ (**16**) respectively. The crystals of **16** were twinned, and refinement did not proceed beyond identifying that the cage was almost identical to that in **15**. Analytical data for both complexes suggest the cobalt core is stable, but that peripheral ligands (e.g., MeCN in **15**) are displaced by water in the bulk.

Complex **15** contains four heterocubanes sharing two Co–O edges and two further Co vertices. The core is shown in Figure 12 and the full structure in Figure 13. The cage

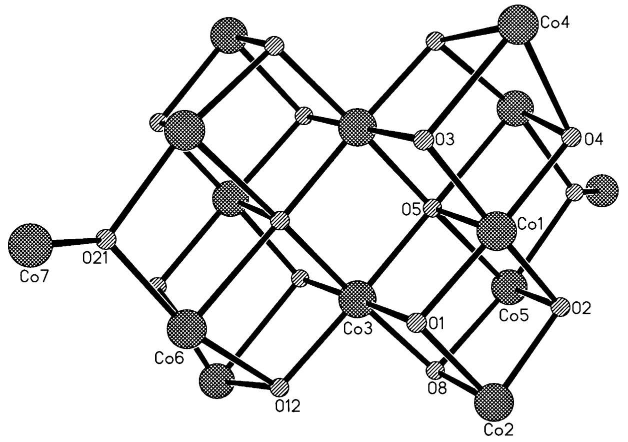

Figure 12. The core of the structure of $[Co_{14}O_4(OH)_{12}(O_2CCMe_3)_{14}(HO_2CCMe_3)_2(H_2O)_6(MeCN)_2]$ (**15**) in the crystal.

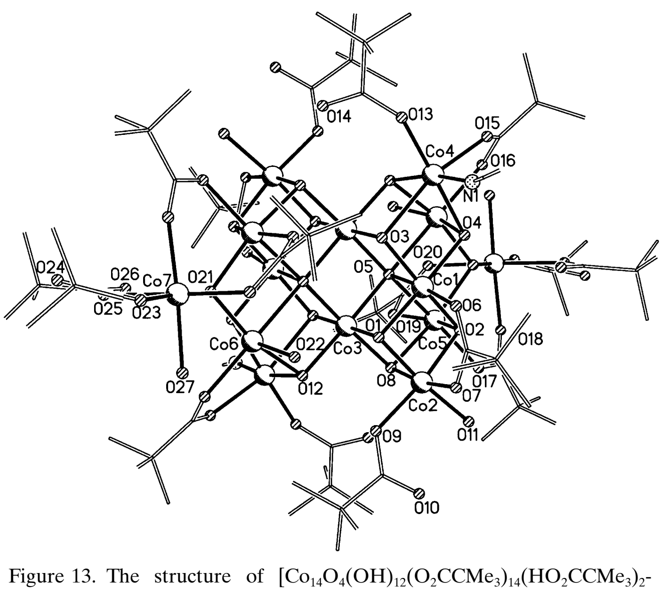

Figure 13. The structure of $[Co_{14}O_4(OH)_{12}(O_2CCMe_3)_{14}(HO_2CCMe_3)_2(H_2O)_6(MeCN)_2]$ (**16**) in the crystal.

crystallises about an inversion centre, and, therefore, there are seven unique cobalt sites. Co1 and O5 (and symmetry equivalents) lie in the shared edges, and Co3 and Co3A are the shared vertices. The four heterocubanes account for twelve Co atoms; the final two Co sites (Co7 and Co7A) are found attached to the periphery through a μ_3-oxide group. This oxide bridges between cubanes, and is not a vertex; the "capping" cobalt atoms are, therefore, attached in a different way to the caps in **11**–**14**. An alternate description would be as a sodium chloride like structure, with cobalt atoms occupying octahedral holes within an oxide structure. In this description, Co3, Co5, Co6 and Co7 and their symmetry equivalents form a central layer with the remaining cobalt sites above and below the layer in the correct place for the extended NaCl lattice.

All the cobalt sites in **15** are six-coordinate. Assigning a precise formula to **15** is difficult. Metric parameters suggest six Co^{III} sites, with bond lengths between 1.866(3) and 1.959(3) Å, and eight Co^{II} sites, with bonds ranging from 1.982(3) to 2.256(3) Å. The bonding of, and likely hydrogen-bonding interactions between, the organic molecules suggests fourteen pivalates and two pivalic acids.

Assigning the single oxygen atoms in the structure presents the difficulty. The two in the shared edge are μ_5-bridging, and therefore clearly oxide. Six more are terminal, and are assigned as water molecules (all involved in two hydrogen bonds). This leaves fourteen μ_3-O atoms to assign. Four are involved in hydrogen bonds to pivalate ligands, and, therefore, must be hydroxide; the alternate assignment as oxide-pivalic acid does not change the overall charge. Six more have metric parameters almost identical to these hydroxides. Two have markedly shorter Co–O bonds, and are assigned as μ_3-oxides. The final two O atoms are intermediate with some long and some short bounds. Charge balance works best if these are hydroxide, which gives: $[Co^{III}_6Co^{II}_8(\mu_5\text{-}O)_2(\mu_3\text{-}O)_2(\mu_3\text{-}OH)_{12}(O_2CCMe_3)_{14}(HO_2CCMe_3)_2(H_2O)_6(MeCN)_2]$. Previously we have shown in chromium(III) clusters[1] that partial protonation of bridging O atoms is possible, and this appears to be another instance in which the presence of both oxide and hydroxide bridges is complicating assignment of oxidation state. The pivalate ligands are divided between 2.11-bridging and terminal ligands; when terminal they form strong intramolecular hydrogen bonds.

Hydrogen bonding: A very large number of hydrogen bonds are found in these structures. In some cases they play a role in stabilising the polymetallic cages. For example, in both **1** and **2** the bridging water molecule has very strong hydrogen bonds to two pivalate ions, while terminal pivalic acid groups hydrogen bond to bridging pivalates. This latter interaction is also found in **7**, **8**, **11** and **13**. Additional molecules of either EtOH or pivalic acid are also found hydrogen bonded to some cages, for example, in **9** and **12**, respectively.

In the crystal lattice for **6** there is a very large amount of hydrogen bonding between co-crystallised pivalate/pivalic acid/water molecules (Figure 14). The hydrogen bonding leads to two separate assemblies. In the first two water and five pivalic acid/pivalates units are linked (Figure 14a). For four of the five organic molecules there is a difference between the two C–O bonds—one short (ca. 1.23 Å) and one long (ca. 1.32 Å)—which suggests the presence of pivalic acid with the H atom involved in the hydrogen bonding. Thus we can assign O30, O31, O34 and O39 as the O–H of the carboxylic acid groups while O29, O32, O33 and O40 as the keto-oxygen atoms. The exception is the molecule containing O35 and O36, whereby the two C–O bonds are almost equivalent (1.26 and 1.27 Å). We therefore assume this is the pivalate ion. This assumption fits well with the pattern of hydrogen bonding, allowing interactions between C-O-H donors and C=O acceptors. O1W acts as an acceptor towards O31, while it donates the H atom in the interaction with O33. O2W interacts with two deprotonated oxygen sites, O29 and O35. There is also a hydrogen bond (2.71 Å) between O1W and O2W. The assembly therefore appears to consist of $[(O_2CCMe_3)(HO_2CCMe_3)_4(H_2O)_2]^-$.

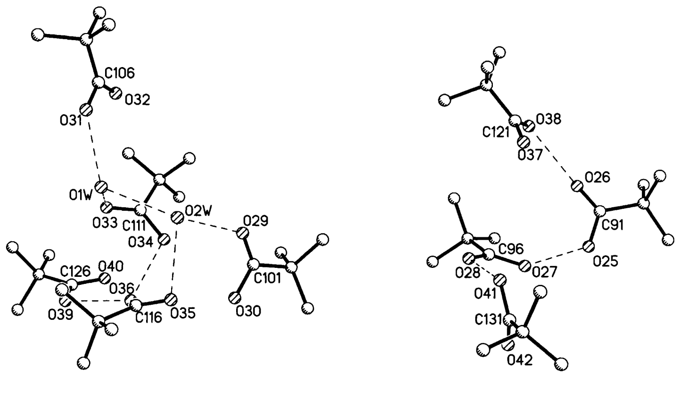

a) b)

Figure 14. The hydrogen bonding in the lattice of **6**: a) an assembly of $[(H_5O_2)(O_2CCMe_3)(HO_2CCMe_3)_4]$ and b) $[(O_2CCMe_3)(HO_2CCMe_3)_3]^-$.

The second assembly contains four pivalic acid/pivalate units, and no water (Figure 14b). Similar arguments to above allows assignment of O25, O38 and O41 as the C-O-H of the acid function, while O26, O37 and O42 belong to the O=C groups. Again, O27 and O28 have very similar C–O bonds lengths (1.25 and 1.28 Å); therefore we should assign this as a pivalate. We can then explain the hydrogen-bonding pattern simply, and the assembly consists of $[(O_2CCMe_3)(HO_2CCMe_3)_3]^-$.

NMR spectroscopy: NMR spectroscopy of paramagnetic compounds constitutes a very rich area of investigation.[11] The interaction between unpaired electrons and any nuclear spin leads to broad (sometimes beyond detection) signals that lack hyperfine structure and are strongly shifted from their diamagnetic positions. While this complicates the interpretation of the spectra, information about the structural, dynamic and electronic properties of the paramagnetic species can sometimes be extracted from the chemical shift and the spin-relaxation time of its nuclei. The complexes presented here appeared suited for NMR characterisation as pivalate contains nine magnetically equivalent protons and confers high solubility on the cages. Preliminary ^1H NMR investigations of **1**–**13**·**14** have been performed with the aim of establishing possible correlations between their solution and solid state structures. A list of the observed chemical shifts is in Table 3.

For complex **1**, only one broad signal at 4.53 ppm is observed in the NMR spectrum, indicating that the solid-state structure is not maintained in solution. The fact that the compound changes color upon dissolution (from pink to violet) supports this conclusion. However, a fluxional process needs to be invoked to account for the high symmetry observed in the NMR timescale. Complex **2** exhibits the analogous behaviour, showing a large broad resonance at 10.90 ppm. For this compound, two paramagnetically shifted signals in the 2:1 intensity ratio are also observed at 0.44 and 20.77 ppm, respectively, which are probably from the pyridine ligands. These arise presumably from the *para* and *meta* positions, respectively. We assume that the *ortho* signals are too broadened for detection, due to the close proximity of these protons to the paramagnetic Co^{II} centers. The alkoxide-bridged complexes **3**, **4** and **5** are not stable in $CDCl_3$, leading to the formation of very fine blue precipitates; this prevents their detection by NMR spectroscopy.

Table 3. ^1H NMR data for complexes **1**–**13**·**14** in $CDCl_3$.

Complex	List of resonances[a,b]
1	4.53
2	0.44 (py, *p*),[c] 10.90, 20.77 (py, *m*)[c]
3, **4**, **5**	complex decomposes in solution
6	0.93, 1.24, 7.35 (H^+),[d] 7.70 (py, *m*),[c] 8.13 (py, *p*),[c] 8.5 (py, *o*)[c]
8	– 24.08, 0.62, ~3,[e] 18.13
9	0.14, 2.87, 13.38
10	– 23.19, 1.28, 7.89, 18.45
11	– 25.07, – 1.01, ~4.6,[e] 17.56
13·**14**	intractable spectrum

[a] The data are given as chemical shift [ppm] on the δ scale. [b] Unless otherwise indicated, all the resonances are assigned to $O_2CCMe_3^-$ or HO_2CCMe_3. [c] py = pyridine, *o* = *ortho*, *m* = *meta*, *p* = *para*. [d] Assigned to the average of protons from HO_2CCMe_3 and H_2O. [e] Obscured by solvent.

Complex **6** is the only cluster in this study in which the Co centers are exclusively in the oxidation state 3+. It is consequently diamagnetic as reflected by its ^1H NMR spectrum (Figure 15, top). In this spectrum, which is consistent with the idealized symmetry (C_{3h}) of the molecule as is revealed by X-ray crystallography, two sharp signals from bound (0.93 ppm) and unbound (1.24 ppm) pivalate are observed. The non-bonded species correspond to one pivalate counterion and 3.5 molecules of pivalic acid per cluster, and are manifested through one unique, averaged resonance. One unique set of signals is observed for the pyridine ligands in form of two triplets (7.70 and 8.13 ppm) and one doublet (8.5 ppm) in the 2:1:2 intensity ratios, respectively. In addition, a broad signal from the acidic protons is present at 7.35 ppm.

Complex **8** shows four signals, the strongest at – 24.08 and 18.13 ppm of approximately equivalent intensity, and two broader peaks at 0.62 and about 3 ppm, respectively (Figure 15, bottom). Surprisingly, the related complex **9** displays a rather different behaviour, with resonances at 0.14, 2.87 and 13.38 ppm. The reasons for this dramatic difference are not clear, the only change being the replacement of one terminal EtOH ligand in **9** by pivalic acid in **8**. Complexes **10** and **11** show a spectrum similar to that obtained from **8**, that is, four distinct resonances within the – 25 to 18 ppm region (Table 3), suggesting that these three compounds converge to a very similar system in solution. The two stronger signals, at approximately – 25 and 18 ppm, might be attributed to two common binding modes for pivalate in this family of clusters, such as μ_2 between Co^{II}–Co^{II} sites and μ_2 between Co^{II}–Co^{III} sites. The complex salt **13**·**14**, formed by two ionic clusters, has a spectrum containing a large number of very weak resonances.

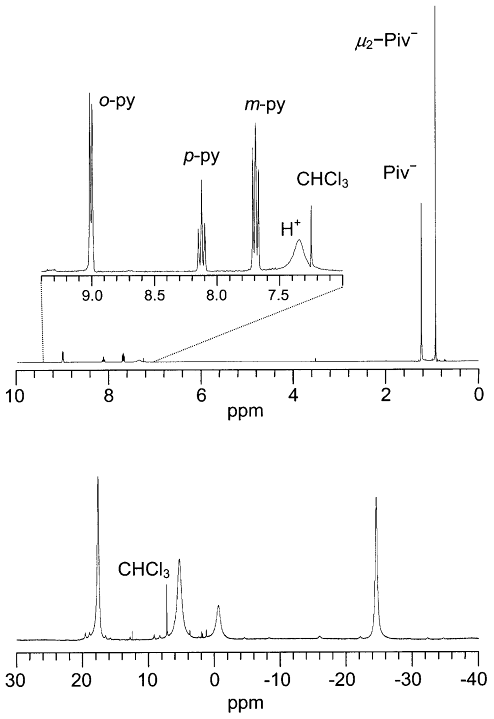

Figure 15. The ^1H NMR spectra of a) **6** and b) **8** recorded in $CDCl_3$ at 300 MHz.

From this spectroscopic study it is concluded that the paramagnetic cobalt aggregates presented in this report do not conserve the symmetry observed in their solid-state structures in solution. This is probably due to the lability of the Co^{II} ion, which in certain cases may involve decomposition of the core of the cluster, and in all cases leads to a fluxional process involving exchange of ligands.

Mass spectroscopy: Electrospray mass spectra were recorded on all clusters in MeCN. In some cases clean spectra were obtained, for others (**2**–**5**, **8**–**10**) little useful information was obtained, presumably reflecting either instability of the clusters in solution or when subjected to the conditions of the ES-MS experiment. Complexes **15** and **16** are beyond the limit of our spectrometer, and no useful information was obtained for either complex. The useful data obtained is listed in Table 4. It is noticeable that no good spectrum is found for any of the homovalent Co^{II} cages, while the homovalent Co^{III} cage gives a very clean spectrum. This reflects the relative

Table 4. Mass spectral data.

	Formula	m/z	Fragment
1	$[Co_2(H_2O)(O_2CCMe_3)_4(HO_2CCMe_3)_4]$	+948	$[M^+]$
6	$[Co_3O(O_2CCMe_3)_6(py)_3]$	+1036	$[M^+]$
		+957	$[M^+ - py]$
7	$[Co_4(OH)_2(O_2CCMe_3)_9(HO_2CCMe_3)_3]$	+1326	$[M^+]$
11	$[Co_6O_2(O_2CCMe_3)_{10}(HO_2CCMe_3)_4]$	+1354	$[M^+ + MeCN]$
12	$[Co_6O_4(O_2CCMe_3)_9(H_2O)_2(HO_2CCMe_3H)_2]$	−1325	$[M^- - H_2O]$
13	$[Co_6O_4(O_2CCMe_3)_9(H_2O)_2]$	−1362	$[M^-]$
14	$[Co_7O_4(O_2CCMe_3)_9(H_2O)_3(MeCN)_2]$	+1508	$[Co_7O_4(O_2CCMe_3)_9(H_2O)^+]$

stabilities of complexes of the two oxidation states. The spectra were obtained in the positive ion mode unless otherwise stated.

Complex **1** has a peak at m/z 948, which fits well with the molecular ion. Higher mass peaks are also observed, which is consistent with the reactivity these cobalt cages show; presumably in solution larger species are forming. The homovalent cobalt(III) cage **6** also has the molecular ion (m/z 1036) and a peak at m/z 957, which corresponds to the loss of one terminal pyridine ligand. Complex **7** has a single peak at m/z 1326, which fits with the molecular ion, while **11** has a large number of peaks around m/z 1354; the peaks are close to the molecular ion, and it appears complex fragmentation is occurring, probably involving MeCN. Complex **12** has a peak for $[M^- - H_2O]$ at m/z 1325, while the complex salt **13**·**14** gives the most satisfying result; in the negative ion spectrum a peak is found at m/z 1362—which fits well with $[M^-]$ for **14**—while in the positive ion spectrum a single peak is found at m/z 1507. This latter peak is a heptanuclear fragment of **13** $[M^+ - 2O_2CCMe_3 - 2H_2O - 2MeCN]$. While the absence of the molecular ion for the cation is disappointing, the very different negative and positive ion spectra support the crystallographic assignment of this as an ion pair.

Discussion

Part of the intent behind this work was to use a combination of metal and ligand that would allow solution reactions to occur, without immediate precipitation of products or interference from solvent, and where characterisation of the solution complexes may be possible. Cobalt was chosen as the metal, because it is known that in one oxidation state (Co^{III}) it forms stable complexes, while as Co^{II} it is highly reactive. We hoped that it may be possible to carry out site specific reactions, performing substitutions at Co^{II} sites, while Co^{III} sites retained their structure. Pivalate was chosen because it makes the clusters soluble in non-coordinating solvents, and because it should be ideal for NMR studies. Other spectroscopic tools, for example, electronic or vibrational spectroscopy, do not give much structural information when polymetallic complexes are involved.

The results are intriguing, and a great deal more complicated than initially expected. The cobalt–pivalate reaction system is extremely rich, with seven different nuclearities found from the reactions performed. The solvent used is vital; protic solvents tend to become involved in the reaction, while the polarity of aprotic solvents can influence whether neutral or charged clusters crystallise. Which clusters are present in solution is not established, with the exception of **6**, which contains exclusively cobalt(III). It is unfortunate that the paramagnetic cages are also those that contain the more reactive oxidation state as this makes it difficult to interpret NMR spectra for precisely those cages for which the nuclearity in solution is questionable. The ES-MS results suggest that the core of the higher nuclearity cages is retained in solution, even if the peripheral ligands are exchanging.

The many structures found suggest a pattern, outlined in Scheme 2. The curious feature is that while hexa- and heptanuclear cages (**12**, **13**, **14**) feature a complete $\{Co_4O_4\}$ cube capped on two or three sites, the $\{Co_5\}$ cages (**8**, **9**) have one vertex of the heterocubane missing, but still two caps. A possible explanation is to derive the structure from addition of a cobalt vertex to the $\{Co_4\}$ rhombus; this hypothesis led us to the remainder of Scheme 2.

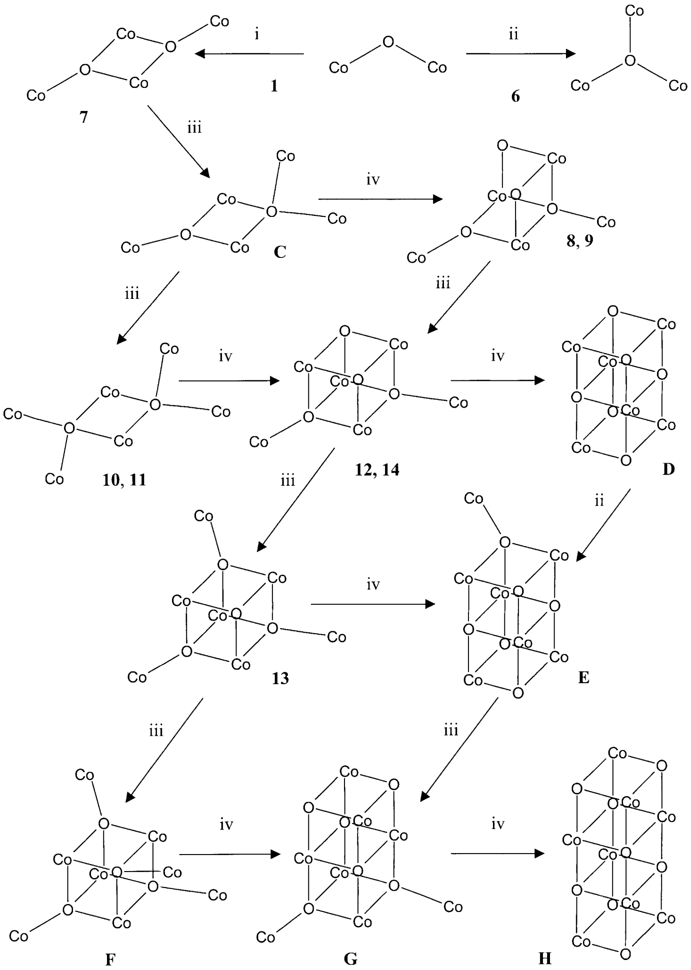

Scheme 2.

Beginning with the dimeric structure **1**, we can have two possible steps—either addition of a cobalt ion and oxidation to the {Co^{III}_3} triangle (process ii in Scheme 2), which reacts no further, or dimerisation to a {Co_4} rhombus (process i in Scheme 2), which can grow metal-by-metal to larger clusters. Two further steps occur—addition of a Co^{II} ion (process iii) or oxidation and concomitant addition of oxide (process iv). Once oxidised to all Co^{III}, it appears the cages are stable (e.g., **6**), and in the heterovalent cages the oxidised core appears unreactive, with growth and oxidation steps occurring at the Co^{II} exterior.

Scheme 2 includes all the structures other than the methoxide-bridged cubane **3**. It also leads us to propose other cages should be present in the reaction, or which should be accessible through this or related chemistry. Some of these putative cores are related to known compounds. The clearest examples are **F** and **H**, both of which are cores known for cobalt. The core of **F** has been reported by Christou and co-workers,[12] with benzoate as the ligand; while the core of **H** has been reported by both the Christou group[13] and Beattie et al.[14]In both of these cages the carboxylate present is acetate. The core of **C** has been found in heterometallic pentanuclear cages made by Timco and co-workers,[15] and the core of **D** has been found in a {Ni_{11}} cage reported by Brechin et al.[16] The only cores for which we are unaware of precedent are **E** and **G**.

Scheme 2 also suggests further growth sequences. For example, we have reported a dodecanuclear Cr^{III} cage,[17] which features a face-sharing triple-cubane capped on the four external oxide sites; that is, core **H** capped in the manner of **F**. Isolation of the intermediate nuclearities with capped-cubane structures, either for cobalt or other metal ions, would support the proposal.

The tetradecanuclear cages **15** and **16** do not readily conform to this pattern. Our present hypothesis is that these are formed from "dimerisation" of a heptanuclear cage, rather than by stepwise addition of cobalt atoms. This suggests that as the clusters grow bond formation between clusters becomes a competitive process with atom by atom growth. This is unsurprising, and similar to growth of colloids of either metals or metal oxides.

Conclusion

The cobalt–pivalate system is remarkably fecund. This is probably because of the very high solubility of the cages, which allows slow reactions to take place before insoluble precipitates form. The many structures have allowed us to "map" the many possible products, and to propose a growth sequence for these cages (Scheme 2). Whether this sequence can be generalised or extended remains to be proven.

Valence bond analysis has been useful in assigning oxidation states of cobalt sites in the various clusters, and with one, disordered, exception matches well expectations from charge balance. It is generally the case that the higher oxidation state is found near the centre of the cluster, with lower oxidation states on the periphery. This suggests that heterometallic cages could be targeted, using +3 ions at the centre decorated with +2 ions on the periphery.

Experimental Section

Preparation of compounds: All reagents, metal salts and ligands were used as obtained from Aldrich. Analytical data, listed in Table 1, were obtained by the microanalytical service of the University of Manchester. Mass spectra, data listed in Table 4, were obtained by electrospray techniques on a using a 30 V cone voltage in MeCN as the carrier phase. All manipulations in the synthesis of compounds **1**, **2** and **A** were carried out under a nitrogen atmosphere.

[$Co_2(\mu\text{-}OH_2)(O_2CCMe_3)_4(HO_2CCMe_3)_4$] (1): Cobalt carbonate (4.0 g, 34 mmol) was treated with an excess of pivalic acid (20.0 g, 196 mmol) in the presence of water (3 mL) at 100 °C for 24 h, leading to dissolution of the carbonate salt. The solution was cooled to room temperature, MeCN (50 mL) was added and the mixture stirred briefly. The solution was filtered and cooled to 5 °C, giving pink crystals of **1** suitable for X ray analyses in one day. The solution was then cooled to −18 °C for 2 days to give a second crop of **1**. The second crop was collected by filtration, washed with cold MeCN and dried in a slow flow of N_2. Complex **1** has a high solubility at room temperature in a wide range of organic solvents (from MeCN to pentane) giving a violet unstable solution. Complex **1** dissolves in H_2O to give a pink solution. Yield: 65.8 %, 10.5 g.

[$Co_2(\mu\text{-}OH_2)(O_2CCMe_3)_4(HO_2CCMe_3)_2(py)_2$] (2): Compound **1** (1.00 g, 1.05 mmol) and pivalic acid (1.50 g, 14.7 mmol) were dissolved in MeCN (5 mL) at room temperature, then pyridine (0.5 g, 6.32 mmol) was added. The solution was cooled to 5 °C, giving pink crystals of **2** that were collected after 2 days by filtration, then washed with cold MeCN. Yield: 38.9 %, 0.37g.

[$Co(O_2CCMe_3)_2]_n$ (A): Compound **1** (3.0 g, 3.2 mmol) was heated to 180 °C under a flow of nitrogen during which time the sample changed colour from pink to violet, and decomposed to give a microcrystalline solid. Yield: 99.3 % 1.64 g. From TG/DTA investigation between 25 °C to 600 °C in a flow of N_2, **1** loses 45 % of its weight on heating to 108 °C, which represents loss of one H_2O and four pivalic acid molecules (calcd 44.95 %) to give the formula of **A**. Little further weight is lost until 270 °C, at which point the residual sample sublimes.

[$Co_4(\mu_3\text{-}OMe)_4(O_2CCMe_3)_4(MeOH)_4$] · 4.5 MeOH (3 · 4.5 MeOH): Compound **A** (0.5 g, 1.9 mmol) was dissolved in MeOH (3.0 mL) at room temperature, and the solution allowed to stand at room temperature. Crystals of **3** begin to form after 0.5 h. Complex **3** was collected by filtration after 2 days and washed with cold MeOH. The crystals very easily lose the solvate of crystallisation. Yield for **3**: 32.8 %, 0.14 g.

[$Co_4(\mu_3\text{-}OH)_2(O_2CCMe_3)_6(EtOH)_6$] · 2 EtOH (4 · 2 EtOH): Complex **A** (0.5 g, 1.9 mmol) was dissolved in EtOH (10.0 mL) at 35–40 °C, and the solution allowed to stand at 5 °C. Crystals of **4** began to form after 1 h. Complex **4** was collected by filtration after 2 days and washed with cold EtOH. Yield: 25.2 %, 0.15 g.

[$Co_4(\mu_3\text{-}OH)_2(O_2CCMe_3)_6(nPrOH)_6$] · 2 PrOH (5 · 2 PrOH): Complex **A** (0.5 g, 1.9 mmol) was dissolved in *n*PrOH (3.0 mL) at 35–40 °C, and the solution was cooled to 5 °C. Pink crystals of **5** were collected by filtration after 2 days and washed with cold *n*PrOH. The crystals very easily lose the solvate of crystallisation and the % yield is calculated excluding lattice solvent. Yield: 20.3 %, 0.12 g.

[$Co_3(\mu_3\text{-}O)(O_2CCMe_3)_6(py)_3$] · O_2CCMe_3 · H_2O · 3.5 HO_2CCMe_3 (6 · O_2CCMe_3 · H_2O · 3.5 HO_2CCMe_3): Complex **1** (4.0 g, 4.2 mmol) was dissolved in pyridine (2.0 g, 25.3 mmol) and pivalic acid (20.0 g, 195.8 mmol) at 80 °C. Air was passed through the solution during 7 h, which changed colour from pink to brown and large dark brown crystals of **6** formed. The crystals were collected by filtration and washed with CCl_4. Yield: 40.0 %, 1.70 g.

[$Co_4(\mu_3\text{-}OH)_2(O_2CCMe_3)_9(HO_2CCMe_3)$] · MeCN (7 · MeCN): Complex **1** (4.0 g, 4.2 mmol) was dissolved in pivalic acid (20.0 g, 195.8 mmol) and MeCN (75 mL) at 60° C. Air was passed through the solution during 72 h, which changed colour from violet to green brown; brown crystals of **7** suitable for X-ray study are deposited during this time. The solution was allowed to cool to room temperature and a product, **B**, was collected by filtration after 1 day and washed with CH_3CN until the washings became green. Yield: 1.1 g. A pure sample of **7** could not be obtained.

[$Co_5(\mu_3\text{-}OH)_2(\mu\text{-}OEt)_2(O_2CCMe_3)_8(HO_2CCMe_3)(EtOH)_3$] · HO_2CCMe_3 (8 · HO_2CCMe_3): Complex **A** (0.5 g, 1.9 mmol) was dissolved in EtOH (10.0 mL) at 35–40 °C, and the solution allowed to stand at room

Table 5. Experimental data for the X-ray studies of **1** – **15**.

	1	**2**	**3**	**4**	**5**
formula	$C_{40}H_{78}Cl_8Co_2O_{17}$	$C_{40}H_{68}Co_2N_2O_{13}$	$C_{28}H_{64}Co_4O_{16} \cdot 4.5\,CH_4O$	$C_{42}H_{92}Co_4O_{20} \cdot 2\,C_2H_6O$	$C_{48}H_{104}Co_4O_{20} \cdot 2\,C_3H_8O$
M	948.9	902.8	1036.7	1245.0	1357.2
crystal system	monoclinic	monoclinic	orthorhombic	monoclinic	triclinic
space group	$P2_1/n$	$C2/c$	$Pbca$	$P2_1/n$	$P\bar{1}$
a [Å]	12.149(4)	24.715(2)	16.019(3)	12.745(6)	12.470(2)
b [Å]	20.027(7)	19.5088(19)	15.450(3)	13.920(7)	13.126(2)
c [Å]	23.097(8)	9.8201(10)	42.279(8)	18.571(9)	13.793(2)
α [°]	90	90	90	90	115.79(1)
β [°]	103.410(7)	96.725(2)	90	92.540(10)	114.01(1)
γ [°]	90	90	90	90	93.39(1)
V [Å^3]	5466(3)	4702.2(8)	10463(3)	3291(3)	1778.7(5)
T [K]	220.0(2)	150.0(2)	150.0(2)	220.0(2)	120.0(2)
Z	4	4[c]	8	2[d]	1[d]
ρ_{calcd} [g^{-1}cm^{-3}]	1.153	1.275	1.316	1.256	1.267
shape and colour	pink block	red block	pink lath	pink block	pink rhomb
size [mm]	0.40 × 0.18 × 0.08	0.32 × 0.14 × 0.14	0.42 × 0.15 × 0.06	0.23 × 0.21 × 0.19	0.45 × 0.25 × 0.15
μ [mm^{-1}]	0.665	0.764	1.310	1.054	0.981
unique data	11138	4786	13139	6681	9979
absorption correction	Sadabs[7]	Sadabs[7]	Sadabs[7]	Sadabs[7]	none
transmission max/min	0.928/0.783	1.000/0.753	0.928/0.621	0.928/0.655	
unique data [$F_o > 4\sigma(F_o)$]	8308	4037	8546	5167	7999
parameters/restraints	754/2400	394/0	532/30	365/77	426/0
$R1/wR2$[a]	0.0454/0.1420	0.0262/0.0659	0.0477/0.1433	0.0807/0.2623	0.0352/0.0980
weighting scheme[b] [w^{-1}]	$\sigma^2(F_o^2) + (0.0873\,P)^2$	$\sigma^2(F_o^2) + (0.0450\,P)^2$	$\sigma^2(F_o^2) + (0.0780\,P)^2 + 0.1307\,P$	$\sigma^2(F_o^2) + (0.0854\,P)^2 + 20.0045\,P$	$\sigma^2(F_o^2) + (0.0618\,P)^2$
goodness of fit	1.077	0.946	1.063	1.169	1.026
largest residuals [e Å^{-3}]	+0.470/−0.492	+0.356/−0.242	+0.662/−0.519	+1.118/−0.618	+0.994/−0.389
	6	**7**	**8**	**9**	**10**
formula	$2\,C_{45}H_{69}Co_3N_3O_{13} \cdot H_5O_2 \cdot 2\,C_5H_9O_2 \cdot 7\,C_5H_{10}O_2$	$C_{50}H_{92}Co_4O_{22} \cdot 0.5\,C_5H_{12}$	$C_{55}H_{112}Co_5O_{25} \cdot C_5H_{10}O_2$	$C_{52}H_{108}Co_5O_{24} \cdot 2\,C_2H_6O$	$C_{58}H_{106}Co_6O_{26} \cdot 0.5\,C_4H_8O_2$
M	3026.8	1317.0	1570.2	1504.2	1617.1
crystal system	orthorhombic	monoclinic	monoclinic	monoclinic	tetragonal
space group	$Pca2_1$	$P2_1/n$	$P2_1/c$	$P2_1/c$	$P\bar{4}n2$
a [Å]	25.392(8)	15.670(4)	15.709(4)	17.205(4)	22.295(5)
b [Å]	25.853(8)	18.882(5)	18.629(5)	15.612(4)	$= a$
c [Å]	24.736(8)	23.575(6)	28.307(8)	29.818(7)	15.127(3)
α [°]	90	90	90	90	90
β [°]	90	98.83(1)	103.23(1)	99.45(1)	90
γ [°]	90	90	90	90	90
V [Å^3]	16238(9)	6893(3)	8064(4)	7901(3)	7519(3)
T [K]	120.0(2)	120.0(2)	120.0(2)	120.0(2)	120.0(2)
Z	4	4	4	4	4[c]
ρ_{calcd} [g^{-1}cm^{-3}]	1.238	1.269	1.293	1.265	1.428
shape and colour	green-black block	black block	green block	green plate	purple prism
size [mm]	0.26 × 0.28 × 0.30	0.60 × 0.30 × 0.20	0.23 × 0.20 × 0.10	0.37 × 0.36 × 0.08	0.50 × 0.18 × 0.15
μ [mm^{-1}]	0.674	1.011	1.076	1.094	1.367
unique data	28597	12148	21388	20957	10917
absorption correction	Sadabs[7]	integration	Sadabs[7]	integration	integration
transmission max/min	0.858/0.828	0.823/0.582	0.900/0.821	0.916/0.726	0.836/0.598
unique data [$F_o > 4\sigma(F_o)$]	24142	9927	12765	15815	9481
parameters/restraints	1717/1	744/37	862/60	903/13	464/2
$R1/wR2$[a]	0.0671/0.1976	0.0609/0.2050	0.0534/0.1337	0.0475/0.1237	0.0307/0.0721
weighting scheme[b] [w^{-1}]	$\sigma^2(F_o^2) + (0.1000\,P)^2 + 5.07\,P$	$\sigma^2(F_o^2) + (0.0871\,P)^2 + 2.203\,P$	$\sigma^2(F_o^2) + (0.0409\,P)^2 + 11.8653\,P$	$\sigma^2(F_o^2) + (0.0493\,P)^2 + 0.9666\,P$	$\sigma^2(F_o^2) + (0.0445\,P)^2$
goodness of fit	1.364	1.661	1.029	1.310	0.985
largest residuals [e Å^{-3}]	+1.257/−0.845	+1.192/−1.188	+0.791/−0.657	+0.897/−0.714	+0.597/−0.270

[a] $R1$ based on observed data, $wR2$ on all unique data. [b] $P = ⅓[\max(F_o^2, 0) + 2F_c]$. [c] The molecule lies on a twofold axis. [d] The molecules lies on an inversion centre. [e] There are two molecules in the asymmetric unit.

temperature in a flask for 2 years, during which time the solution changed colour from violet to green and green crystals suitable for X-ray study were formed. Yield: 18.3 %, 0.11 g.

$[Co_5(\mu_3\text{-}OH)_2(\mu\text{-}OEt)_2(O_2CCMe_3)_8(EtOH)_4] \cdot 2\,EtOH$ (9 · 2 EtOH): Complex **10** (1.00 g, 0.62 mmol) was dissolved in ethanol (10 mL) at room temperature and the solution allowed to stand at room temperature for three days and then left to stand at −30°. Green crystals of **9** formed in 5 days, and were collected by filtration after 2 weeks and washed with cold EtOH. The crystals very easily lose the solvate of crystallisation. Yield calculated for **9**: 19.7 %, 0.22 g.

$[Co_6(\mu_4\text{-}O)_2(O_2CCMe_3)_{10}(EtOAc)_2] \cdot 0.5\,EtOAc$ (10 · 0.5 EtOAc): Complex **B** (1.00 g, 0.84 mmol) was dissolved in ethyl acetate (30 mL) at room

Table 5. (cont.)

	11	**12**	**13·14**	**15**
formula	$C_{70}H_{130}Co_6O_{30}\cdot 0.25\,C_4H_8O_2$	$C_{16}H_{36}N\cdot C_{45}H_{85}Co_6O_{24}\cdot 2\,C_5H_{10}O_2\cdot 3\,CH_3NO_2$	$C_{54}H_{103}Co_7N_2O_{27}\cdot C_{45}H_{85}Co_6O_{24}\cdot 2.5\,C_5H_{10}O_2\cdot 3.5\,C_2H_3N\cdot 2.5\,H_2O$	$C_{84}H_{154}Co_{14}N_2O_{54}\cdot 2\,C_2H_3N\cdot 4\,H_2O$
M	1827.4	1866.3	3432.7	3035.3
crystal system	triclinic	triclinic	triclinic	monoclinic
space group	$P\bar{1}$	$P\bar{1}$	$P\bar{1}$	$P2_1/n$
a [Å]	15.653(3)	14.988(4)	15.971(3)	14.0661(19)
b [Å]	22.664(5)	15.958(5)	21.979(4)	25.130(4)
c [Å]	28.887(6)	22.907(6)	24.837(5)	19.809(7)
α [°]	109.19(1)	77.626(9)	76.37(1)	90
β [°]	104.60(1)	89.268(7)	79.89(1)	104.712(2)
γ [°]	94.55(1)	74.794(6)	84.91(1)	90
V [Å^3]	9217(3)	5159(3)	8331(3)	6772(2)
T [K]	120.0(2)	100.0(2)	120.0(2)	100(2)
Z	4[e]	2	2	2[c]
ρ_{calcd} [g^{-1} cm^{-3}]	1.317	1.201	1.368	1.489
shape and colour	bronze plate	dark green lath	dark green trapezoid	black prisms
size [mm]	0.34 × 0.20 × 0.07	0.30 × 0.20 × 0.10	0.40 × 0.10 × 0.05	0.55 × 0.30 × 0.25
μ [mm^{-1}]	1.126	1.310	1.336	1.749
unique data	48085	17807	38282	13639
absorption correction	integration	semiempirical	integration	Sadabs^7
transmission max/min	0.917/0.748	0.906/0.751	0.940/0.618	0.669/0.446
unique data [$F_o > 4\sigma(F_o)$]	33125	12827	25256	10879
parameters/restraints	1964/30	945/459	1851/93	769/0
$R1/wR2$[a]	0.0556/0.1412	0.0785/0.2347	0.0596/0.1858	0.0586/0.1633
weighting scheme[b] [w^{-1}]	$\sigma^2(F_o^2) + (0.0439\,P)^2 + 2.08\,P$	$\sigma^2(F_o^2) + (0.161\,P)^2$	$\sigma^2(F_o^2) + (0.0800\,P)^2$	$\sigma^2(F_o^2) + (0.0960\,P)^2 + 8.399\,P$
goodness of fit	1.283	1.024	1.198	1.052
largest residuals [e Å^{-3}]	+1.206/−0.747	+1.750/−1.120	+1.315/−0.655	+1.776/−1.030

[a] $R1$ based on observed data, $wR2$ on all unique data. [b] $P = \frac{1}{3}[\max(F_o^2, 0) + 2F_c]$. [c] The molecule lies on a twofold axis. [d] The molecules lies on an inversion centre. [e] There are two molecules in the asymmetric unit.

temperature and the solution allowed to stand at room temperature. Crystals of **10** formed the next day, which were collected after 3 days, and washed with EtOAc. Yield (calculated from **1** used to make **B**): 22.8%, 0.47 g.

[$Co_6(\mu_4\text{-}O)_2(O_2CCMe_3)_{10}(HO_2CCMe_3)_4$]·0.25 EtOAc (11·0.25 EtOAc): Complex **1** (3.0 g, 3.2 mmol) was dissolved in MeCN (150 mL). A 0.68 wt% solution of H_2O_2 in water (2.998 g) was dissolved in MeCN (10 mL) and added to the reaction mixture. The solution changed colour from purple to green within a few seconds. After about an hour a small amount of green precipitate was observed to form. This was filtered off and the acetonitrile solution allowed to evaporate to dryness at room temperature. The residue was dissolved in ethyl acetate (50 mL) and left to stand. After five days dark brown/orange crystals of **11** were collected. Yield: 31.4%, 0.60 g.

[$(C_4H_9)_4N$][$Co_6O_4(O_2CCMe_3)_9(H_2O)_2$]·2 HO_2CCMe_3H (12): Complex **1** (2.05 g, 2.0 mmol) was dissolved in MeCN (80 mL) and treated with a solution of tetrabutylammonium permanganate (0.26 g) in MeCN (20 mL). A very dark green solution was obtained which was stirred for three hours and then allowed to evaporate to dryness overnight to give a green gel. The gel was extracted with $MeNO_2$ to give a green solution and a brown residue. The green solution was cooled to −18 °C for eight days after which large green hexagonal crystals of **12** were obtained. Yield: 13.0%, 0.15 g. Electro spray MS showed the molecular ion less water at 1325.

[$Co_7(\mu_4\text{-}O)_3(\mu_3\text{-}O)(O_2CCMe_3)_9(HO_2CCMe_3)(H_2O)_3(MeCN)_2$]·[$Co_6(\mu_4\text{-}O)_2(\mu_3\text{-}O)_2(O_2CCMe_3)_9(H_2O)_2$]·3 Me_3CCO_2H·2 H_2O (13·14·3 Me_3CCO_2H·2 H_2O): Complex **1** (0.60 g 0.63 mmol) was dissolved in acetonitrile (50 mL). 30 wt% hydrogen peroxide solution in water (0.5 mL) was added. The solution changed colour from purple to green within a few seconds. After about an hour a small amount of green precipitate was observed to form and was removed by filtration. Slow evaporation of the filtrate over several days gave dark brown/orange crystals of **13·14** which were collected. Yield: 74%, 0.22 g.

[$Co_{14}O_4(OH)_{12}(O_2CCMe_3)_{14}(HO_2CCMe_3)_2(H_2O)_6(MeCN)_2$] (15): Complex **1** (0.52 g, 0.55 mmol) was dissolved in acetonitrile (25 mL) and treated with *tert*-butylperoxide (1 mL of a 70% aqueous solution, 6.7 mmol). The solution turned from blue to green and a precipitate formed. The precipitate was collected by filtration and dissolved in a 1:1 mixture of MeCN and Et_2O. The solution was allowed to evaporate and after several days small green needles were formed suitable for X-ray study. Yield: 8.0%, 0.02 g.

[$Co_{14}O_4(OH)_{12}(O_2CCMe_3)_{14}(H_2O)_8(HO_2CCMe_3)_3$] (16): Complex **1** (0.52 g, 0.55 mmol) was dissolved in MeCN (50 mL) and potassium dichromate (0.036 g, 0.12 mmol) was added as a solid. The solution gradually turned a deep purple colour and after three days most of the potassium dichromate had dissolved and the solution was brown. On standing for 21 days small dark crystals were obtained. The crystals proved to be twinned, but of sufficient quality to allow the connectivity of the cage to be established. Refinement was not completed due to the poor quality of the data, compared with the better data obtained for the analogous structure **14**. Yield: 30.8%, 0.07 g.

Crystallography: Crystal data and data collection and refinement parameters for compounds **1**–**15** are given in Table 5, selected bond lengths and angles are given in Tables 6–18.

Data collection and processing: Data were collected with a Bruker Smart APEX CCD area detector equipped with an Oxford Cryosystems low-temperature device,[18] using $Mo_{K\alpha}$ radiation: $\omega-\phi$ scans for **1**, **2** and **4**; ω scans for all other structures. Data were corrected for Lorentz and polarisation factors. Absorption corrections were applied to all data, except that for **5**.

Structure analysis and refinement: Structures **2** and **5**–**15** were solved by direct methods using SHELXS-97;[19] structures **1** and **4** were solved by heavy atom methods using DIRDIF;[20] the structure of **3** was solved from the isostructural Ni complex.[21] All structures were completed by iterative cycles of ΔF syntheses and full-matrix least-squares refinement. All non-hydrogen atoms were refined anisotropically in all structures except for: all part-weight C atoms in **6**, **7** and **10**; C atoms with 0.25 occupancy in **8** and with 0.15 and 0.5 occupancy in **9**; atoms of disordered solvent molecules in **6**, **10** and **11**. All hydrogen atoms were located in difference maps, and freely refined in **2**. In all other structures difference Fourier syntheses were employed in positioning idealised methyl-hydrogen atoms, which were

Table 6. Bond lengths [Å] and angles [°] for **1** and **2**.

1		**2**	
Co1−O1E	2.0567(15)	Co1−O1A2	2.0233(9)
Co1−O1D	2.0613(15)	Co1−1A1#1	2.0256(9)
Co1−O12	2.0800(14)	Co1−O1B2	2.1147(9)
Co1−O1C	2.0962(15)	Co1−N11	2.1327(12)
Co1−O1B	2.0992(16)	Co1−O1 H	2.1596(8)
Co1−O1A	2.1274(15)	Co1−O1C2	2.1898(9)
Co2−O2D	2.0376(15)		
Co2−O2E	2.0598(16)		
Co2−O1F	2.0873(15)		
Co2−O12	2.0983(16)		
Co2−O1G	2.1113(17)		
Co2−O1H	2.1330(16)		
O1E-Co1-O1D	93.20(6)	O1A2-Co1-O1A1#1	93.82(4)
O1E-Co1-O12	98.09(6)	O1A2-Co1-O1B2	176.34(4)
O1D-Co1-O12	91.34(6)	O1A1#1-Co1-O1B2	87.36(4)
O1E-Co1-O1C	87.40(6)	O1A2-Co1-N11	88.34(4)
O1D-Co1-O1C	177.99(6)	O1A1#1-Co1-N11	168.57(4)
O12-Co1-O1C	90.47(6)	O1B2-Co1-N11	89.83(4)
O1E-Co1-O1B	86.90(6)	O1A2-Co1-O1 H	94.79(3)
O1D-Co1-O1B	89.18(6)	O1A1#1-Co1-O1 H	94.69(4)
O12-Co1-O1B	174.94(6)	O1B2-Co1-O1 H	88.56(3)
O1C-Co1-O1B	88.94(6)	N11-Co1-O1 H	96.31(4)
O1E-Co1-O1A	173.56(6)	O1A2-Co1-O1C2	89.01(4)
O1D-Co1-O1A	87.82(6)	O1A1#1-Co1-O1C2	83.44(4)
O12-Co1-O1A	88.24(6)	O1B2-Co1-O1C2	87.68(4)
O1C-Co1-O1A	91.37(6)	N11-Co1-O1C2	85.38(4)
O1B-Co1-O1A	86.75(7)	O1 H-Co1-O1C2	175.87(3)
O2D-Co2-O2E	95.84(7)	Co1-O1H-Co1#1	108.44(6)
O2D-Co2-O1F	90.99(7)		
O2E-Co2-O1F	172.05(6)		
O2D-Co2-O12	95.46(5)		
O2E-Co2-O12	91.72(6)		
O1F-Co2-O12	91.67(6)		
O2D-Co2-O1G	91.49(6)		
O2E-Co2-O1G	86.73(6)		
O1F-Co2-O1G	89.04(6)		
O12-Co2-O1G	173.00(6)		
O2D-Co2-O1H	175.05(6)		
O2E-Co2-O1H	87.85(7)		
O1F-Co2-O1H	85.11(6)		
O12-Co2-O1H	87.71(6)		
O1G-Co2-O1H	85.41(6)		
Co1-O12-Co2	110.23(6)		

Table 7. Bond lengths [Å] and angles [°] for **3**.

Co1−O1B	2.0454(18)	Co3−O1D	2.0664(19)
Co1−O123	2.0711(17)	Co3−O123	2.0751(18)
Co1−O124	2.0727(17)	Co3−O31	2.100(2)
Co1−O134	2.0889(18)	Co3−O134	2.1000(18)
Co1−O1A	2.1532(19)	Co3−O234	2.1020(17)
Co1−O2A	2.1767(19)	Co3−O32	2.1177(19)
Co2−O2B	2.0305(18)	Co4−O2D	2.0585(18)
Co2−O234	2.0543(18)	Co4−O124	2.0647(18)
Co2−O123	2.1010(17)	Co4−O41	2.075(2)
Co2−O124	2.1033(17)	Co4−O134	2.0816(18)
Co2−O1C	2.1556(18)	Co4−O234	2.1168(17)
Co2−O2C	2.1889(19)	Co4−O42	2.1555(19)
O1B-Co1-O123	93.52(7)	O1D-Co3-O123	169.35(7)
O1B-Co1-O124	94.04(7)	O1D-Co3-O31	90.68(7)
O123-Co1-O124	89.67(7)	O123-Co3-O31	96.12(7)
O1B-Co1-O134	170.76(7)	O1D-Co3-O134	93.91(7)
O123-Co1-O134	79.85(7)	O123-Co3-O134	79.51(7)
O124-Co1-O134	79.60(7)	O31-Co3-O134	175.26(7)
O1B-Co1-O1A	90.76(7)	O1D-Co3-O234	91.75(7)
O123-Co1-O1A	103.66(7)	O123-Co3-O234	79.66(7)
O124-Co1-O1A	165.54(7)	O31-Co3-O234	93.81(8)
O134-Co1-O1A	97.03(7)	O134-Co3-O234	87.22(7)
O1B-Co1-O2A	90.82(7)	O1D-Co3-O32	90.86(7)
O123-Co1-O2A	163.40(7)	O123-Co3-O32	97.80(7)
O124-Co1-O2A	106.01(7)	O31-Co3-O32	85.68(8)
O134-Co1-O2A	97.34(7)	O134-Co3-O32	93.07(8)
O1A-Co1-O2A	60.23(8)	O234-Co3-O32	177.34(7)
O2B-Co2-O234	171.26(7)	O2D-Co4-O124	169.88(7)
O2B-Co2-O123	93.94(7)	O2D-Co4-O41	90.94(8)
O234-Co2-O123	80.15(7)	O124-Co4-O41	95.26(7)
O2B-Co2-O124	93.42(7)	O2D-Co4-O134	93.95(7)
O234-Co2-O124	80.03(7)	O124-Co4-O134	79.95(7)
O123-Co2-O124	88.05(7)	O41-Co4-O134	175.10(8)
O2B-Co2-O1C	90.11(7)	O2D-Co4-O234	92.26(7)
O234-Co2-O1C	97.49(7)	O124-Co4-O234	79.48(7)
O123-Co2-O1C	103.38(7)	O41-Co4-O234	92.86(8)
O124-Co2-O1C	167.79(7)	O134-Co4-O234	87.31(7)
O2B-Co2-O2C	91.13(7)	O2D-Co4-O42	89.60(7)
O234-Co2-O2C	96.40(7)	O124-Co4-O42	98.76(7)
O123-Co2-O2C	162.65(7)	O41-Co4-O42	86.18(8)
O124-Co2-O2C	108.22(7)	O134-Co4-O42	93.49(8)
O1C-Co2-O2C	59.98(7)	O234-Co4-O42	177.92(7)

Table 8. Bond lengths [Å] and angles [°] for **4** and **5**.

4		**5**	
Co1−O4	2.0341(14)	Co1−O4	2.0325(11)
Co1−O1	2.0447(13)	Co1−O1	2.0663(10)
Co1−O2	2.0932(14)	Co1−O8	2.0944(11)
Co1−O6	2.1298(15)	Co1−O1	2.1069(11)
Co1−O8	2.1426(15)	Co1−O2	2.1124(11)
Co1−O7	2.2656(13)	Co1−O9	2.1608(11)
Co2−O5	2.0287(13)	Co2−O1	2.0370(10)
Co2−O1	2.0772(13)	Co2−O5	2.0381(11)
Co2−O3	2.1083(14)	Co2−O3	2.1012(11)
Co2−O1#1	2.1109(13)	Co2−O10	2.1147(12)
Co2−O10	2.1157(13)	Co2−O6	2.1703(10)
Co2−O9	2.1709(15)	Co2−O7	2.1847(11)
O4-Co1-O1	105.94(5)	O4-Co1-O1	98.62(4)
O4-Co1-O2	92.27(6)	O4-Co1-O8	91.35(5)
O1-Co1-O2	93.01(5)	O1-Co1-O8	169.19(4)
O4-Co1-O6	161.29(5)	O4-Co1-O1	177.65(4)
O1-Co1-O6	92.77(5)	O1-Co1-O1	82.17(4)
O2-Co1-O6	86.75(5)	O8-Co1-O1	87.71(4)
O4-Co1-O8	90.98(6)	O4-Co1-O2	87.49(5)
O1-Co1-O8	87.63(5)	O1-Co1-O2	98.26(4)
O2-Co1-O8	176.38(5)	O8-Co1-O2	86.29(4)
O6-Co1-O8	89.66(6)	O1-Co1-O2	94.59(4)
O4-Co1-O7	101.94(5)	O4-Co1-O9	86.93(5)
O1-Co1-O7	151.51(5)	O1-Co1-O9	87.12(4)
O2-Co1-O7	91.60(5)	O8-Co1-O9	89.26(5)
O6-Co1-O7	59.44(5)	O1-Co1-O9	90.91(4)
O8-Co1-O7	86.17(5)	O2-Co1-O9	172.78(4)
O5-Co2-O1	97.41(6)	O1-Co2-O5	102.90(4)
O5-Co2-O3	91.12(5)	O1-Co2-O3	91.44(4)
O1-Co2-O3	97.66(5)	O5-Co2-O3	92.94(4)
O5-Co2-O1#1	177.89(5)	O1-Co2-O10	90.03(4)
O1-Co2-O1#1	81.63(5)	O5-Co2-O10	90.16(5)
O3-Co2-O1#1	90.88(5)	O3-Co2-O10	176.20(4)
O5-Co2-O10	89.33(6)	O1-Co2-O6	155.58(4)
O1-Co2-O10	169.99(5)	O5-Co2-O6	101.52(4)
O3-Co2-O10	89.56(5)	O3-Co2-O6	87.81(4)
O1#1-Co2-O10	91.38(5)	O10-Co2-O6	89.41(4)
O5-Co2-O9	87.12(5)	O1-Co2-O7	95.49(4)
O1-Co2-O9	88.10(5)	O5-Co2-O7	161.57(4)
O3-Co2-O9	174.15(5)	O3-Co2-O7	85.27(4)
O1#1-Co2-O9	90.96(5)	O10-Co2-O7	91.10(4)
O10-Co2-O9	84.84(5)	O6-Co2-O7	60.12(4)
Co1-O1-Co2	107.51(6)	Co2-O1-Co1	109.01(5)
Co1-O1-Co2#1	129.60(6)	Co2-O1-Co1	128.95(5)

Table 9. Bond lengths [Å] and angles [°] for **6**.

Co1−O01	1.861(4)	Co2−O11A	1.911(7)
Co1−O1A	1.900(8)	Co2−O9A	1.933(7)
Co1−O12A	1.918(7)	Co2−N2	2.004(5)
Co1−O10A	1.935(7)	Co3−O01	1.866(4)
Co1−O3A	1.957(9)	Co3−O4A	1.884(9)
Co1−N1	2.001(5)	Co3−O2A	1.893(8)
Co2−O01	1.835(4)	Co3−O6A	1.917(9)
Co2−O5A	1.897(9)	Co3−O7A	1.920(8)
Co2−O8A	1.904(9)	Co3−N3	2.003(4)
O01-Co1-O1A	92.7(3)	O8A-Co2-O9A	160.0(4)
O01-Co1-O12A	95.4(2)	O11A-Co2-O9A	93.5(4)
O1A-Co1-O12A	159.6(4)	O01-Co2-N2	179.5(2)
O01-Co1-O10A	92.0(2)	O5A-Co2-N2	84.6(3)
O1A-Co1-O10A	69.1(4)	O8A-Co2-N2	86.9(3)
O12A-Co1-O10A	91.9(4)	O11A-Co2-N2	84.8(3)
O01-Co1-O3A	95.6(3)	O9A-Co2-N2	84.3(2)
O1A-Co1-O3A	92.9(4)	O01-Co3-O4A	94.3(3)
O12A-Co1-O3A	104.9(4)	O01-Co3-O2A	95.7(3)
O10A-Co1-O3A	160.8(4)	O4A-Co3-O2A	93.3(4)
O01-Co1-N1	179.6(2)	O01-Co3-O6A	93.3(3)
O1A-Co1-N1	87.0(3)	O4A-Co3-O6A	172.3(4)
O12A-Co1-N1	84.9(2)	O2A-Co3-O6A	86.9(4)
O10A-Co1-N1	87.7(3)	O01-Co3-O7A	96.4(3)
O3A-Co1-N1	84.7(3)	O4A-Co3-O7A	88.1(4)
O01-Co2-O5A	95.7(3)	O2A-Co3-O7A	167.7(4)
O01-Co2-O8A	92.7(3)	O6A-Co3-O7A	90.1(4)
O5A-Co2-O8A	93.8(5)	O01-Co3-N3	178.91(18)
O01-Co2-O11A	94.8(2)	O4A-Co3-N3	86.5(3)
O5A-Co2-O11A	159.2(4)	O2A-Co3-N3	83.4(3)
O8A-Co2-O11A	67.8(4)	O6A-Co3-N3	86.0(3)
O01-Co2-O9A	96.0(2)	O7A-Co3-N3	84.5(3)
O5A-Co2-O9A	103.2(4)	Co2-O01-Co1	120.79(19)
Co1-O01-Co3	118.93(19)	Co2-O01-Co3	120.24(19)

Table 10. Bond lengths [Å] and angles [°] for **7**.

Co1−O02	1.803(3)	Co2−O02	1.802(3)
Co1−O9	1.888(3)	Co2−O13	1.893(3)
Co1−O1	1.897(3)	Co2−O11	1.893(3)
Co1−O01	1.904(3)	Co2−O2	1.908(3)
Co1−O3	1.917(3)	Co2−O01	1.908(3)
Co1−O7	1.918(3)	Co2−O5A	1.936(4)
Co3−O6A	1.879(4)	Co4−O02	1.797(3)
Co3−O15A	1.887(3)	Co4−O10	1.901(3)
Co3−O4	1.908(3)	Co4−O12	1.901(3)
Co3−O16A	1.922(4)	Co4−O14	1.903(3)
Co3−O01	1.942(3)	Co4−O8	1.922(3)
Co3−O17A	1.964(4)	Co4−O19A	2.015(6)
O02-Co1-O9	98.03(13)	O02-Co2-O13	92.38(13)
O02-Co1-O1	88.78(13)	O02-Co2-O11	97.79(13)
O9-Co1-O1	172.98(13)	O13-Co2-O11	90.23(15)
O02-Co1-O01	82.73(12)	O02-Co2-O2	87.19(13)
O9-Co1-O01	91.12(12)	O13-Co2-O2	87.27(14)
O1-Co1-O01	91.43(11)	O11-Co2-O2	174.52(13)
O02-Co1-O3	176.33(12)	O02-Co2-O01	82.66(12)
O9-Co1-O3	85.63(12)	O13-Co2-O01	174.94(13)
O1-Co1-O3	87.58(13)	O11-Co2-O01	89.46(13)
O01-Co1-O3	96.89(12)	O2-Co2-O01	93.46(12)
O02-Co1-O7	91.01(12)	O02-Co2-O5A	173.23(18)
O9-Co1-O7	90.75(12)	O13-Co2-O5A	89.29(16)
O1-Co1-O7	87.42(12)	O11-Co2-O5A	88.76(18)
O01-Co1-O7	173.66(12)	O2-Co2-O5A	86.34(17)
O3-Co1-O7	89.29(12)	O01-Co2-O5A	95.75(15)
O6A-Co3-O15A	92.73(15)	O02-Co4-O10	100.22(12)
O6A-Co3-O4	173.85(15)	O02-Co4-O12	99.99(13)
O15A-Co3-O4	87.77(15)	O10-Co4-O12	88.52(14)
O6A-Co3-O16A	88.44(16)	O02-Co4-O14	87.49(14)
O15A-Co3-O16A	68.64(15)	O10-Co4-O14	172.20(15)
O4-Co3-O16A	86.04(14)	O12-Co4-O14	88.94(15)
O6A-Co3-O01	89.69(14)	O02-Co4-O8	86.73(13)
O15A-Co3-O01	107.38(13)	O10-Co4-O8	88.22(13)
O4-Co3-O01	96.01(12)	O12-Co4-O8	172.96(14)
O16A-Co3-O01	175.50(14)	O14-Co4-O8	93.47(14)
O6A-Co3-O17A	88.63(18)	O02-Co4-O19A	178.1(2)
O15A-Co3-O17A	162.14(16)	O10-Co4-O19A	81.4(2)
O4-Co3-O17A	89.03(18)	O12-Co4-O19A	81.01(19)
O16A-Co3-O17A	93.62(17)	O14-Co4-O19A	90.9(2)
O01-Co3-O17A	90.43(15)	O8-Co4-O19A	92.33(19)
Co1-O01-Co2	92.50(11)	Co4-O02-Co2	123.30(16)
Co1-O01-Co3	125.00(14)	Co4-O02-Co1	123.43(15)
Co2-O01-Co3	122.66(14)	Co2-O02-Co1	99.64(13)

Table 11. Bond lengths [Å] for **8** and **9**.

8		**9**	
Co1−O10	2.050(3)	Co1−O7	2.030(2)
Co1−O5	2.066(3)	Co1−O3	2.066(2)
Co1−O8	2.066(3)	Co1−O5	2.0751(19)
Co1−O3	2.090(3)	Co1−O1	2.0773(17)
Co1−O1	2.107(3)	Co1−O19	2.106(2)
Co1−O7	2.115(3)	Co1−O20	2.165(2)
Co2−O12	1.885(2)	Co2−O6	1.8968(18)
Co2−O9	1.899(3)	Co2−O22	1.8979(17)
Co2−O6	1.902(2)	Co2−O4	1.9013(18)
Co2−O10	1.905(2)	Co2−O1	1.9048(18)
Co2−O14	1.918(2)	Co2−O9	1.9097(18)
Co2−O11	1.923(2)	Co2−O21	1.9268(17)
Co3−O17	2.017(3)	Co3−O8	2.0217(18)
Co3−O4	2.034(3)	Co3−O11	2.0357(19)
Co3−O13	2.080(3)	Co3−O1	2.0993(17)
Co3−O10	2.097(3)	Co3−O2	2.1296(18)
Co3−O16	2.221(3)	Co3−O23	2.178(2)
Co3−O11	2.235(2)	Co3−O21	2.2455(18)
Co4−O13	1.887(2)	Co4−O2	1.8944(19)
Co4−O21	1.892(3)	Co4−O15	1.8974(18)
Co4−O12	1.894(2)	Co4−O13	1.9005(18)
Co4−O19	1.902(3)	Co4−O22	1.9011(17)
Co4−O15	1.924(2)	Co4−O21	1.9309(17)
Co4−O11	1.937(2)	Co4−O10	1.9319(18)
Co5−O18	2.037(3)	Co5−O16	2.035(2)
Co5−O13	2.043(3)	Co5−O14	2.074(2)
Co5−O25	2.059(3)	Co5−O2	2.0860(18)
Co5−O22	2.076(3)	Co5−O17	2.0893(19)
Co5−O20	2.076(3)	Co5−O24	2.097(2)
Co5−O23	2.251(3)	Co5−O12	2.129(3)

assigned isotropic thermal parameters ($U(\mathrm{H}) = 1.5\,U_{\mathrm{eq}}(\mathrm{C})$ in **1**, **3**, **4**, **12** and **15**) or a common isotropic thermal parameter (in **5**–**11** and **13**.**14**), and allowed to ride on their parent C atoms (C−H 0.93 Å). OH atoms were located and refined in **1**, **4**, **5** and **6**.

Some or all of the pivalate groups in each of **5**–**15** show rotational disorder. Details of the disorder, and modelling strategies used are given in the supplementary crystallographic data deposited at CCDC (see below). In **7** two pivalate ligands are disordered between two positions in a 3:1 ratio; for one of these pivalates the coordination mode is different in the two positions—bidentate for the major component and monodentate for the minor (see Results section for full discussion). For **11** the first of two hexanuclear clusters in the asymmetric unit (i.e., Co1–Co6) is superimposed on its mirror image in a ratio of 93.6:6.4. Of the minor component only Co1′, Co2′, Co5′ and Co6′ could be located; they were refined isotropically. For **13**·**14** one carboxylate group was disordered over two orientations, and there was a large amount of disordered solvent in the lattice. All refinements were against F^2 and used SHELXL-97.[19]

Table 12. Selected bond angles [°] for **8** and **9**.

8		**9**	
O10-Co1-O5	97.08(10)	O7-Co1-O3	177.60(9)
O10-Co1-O8	83.99(11)	O7-Co1-O5	92.35(9)
O5-Co1-O8	90.71(11)	O3-Co1-O5	90.04(9)
O10-Co1-O3	97.95(11)	O7-Co1-O1	95.02(8)
O5-Co1-O3	87.19(11)	O3-Co1-O1	84.94(8)
O8-Co1-O3	177.29(12)	O5-Co1-O1	94.83(7)
O10-Co1-O1	170.68(11)	O7-Co1-O19	90.61(9)
O5-Co1-O1	88.41(11)	O3-Co1-O19	89.30(9)
O8-Co1-O1	88.43(11)	O5-Co1-O19	88.16(8)
O3-Co1-O1	89.80(11)	O1-Co1-O19	173.50(8)
O10-Co1-O7	86.38(11)	O7-Co1-O20	88.45(9)
O5-Co1-O7	175.11(11)	O3-Co1-O20	89.15(8)
O8-Co1-O7	93.10(12)	O5-Co1-O20	173.40(8)
O3-Co1-O7	88.91(12)	O1-Co1-O20	91.63(8)
O1-Co1-O7	88.62(12)	O19-Co1-O20	85.27(9)
O12-Co2-O9	93.14(11)	O6-Co2-O22	174.68(8)
O12-Co2-O6	175.38(11)	O6-Co2-O4	90.50(8)
O9-Co2-O6	90.85(11)	O22-Co2-O4	94.13(8)
O12-Co2-O10	85.39(11)	O6-Co2-O1	97.18(8)
O9-Co2-O10	97.44(11)	O22-Co2-O1	84.85(8)
O6-Co2-O10	96.41(11)	O4-Co2-O1	97.15(8)
O12-Co2-O14	90.22(10)	O6-Co2-O9	86.60(8)
O9-Co2-O14	86.97(11)	O22-Co2-O9	91.18(8)
O6-Co2-O14	87.67(10)	O4-Co2-O9	85.27(8)
O10-Co2-O14	173.92(11)	O1-Co2-O9	175.48(7)
O12-Co2-O11	85.05(10)	O6-Co2-O21	91.44(7)
O9-Co2-O11	177.20(11)	O22-Co2-O21	83.78(7)
O6-Co2-O11	90.87(10)	O4-Co2-O21	176.08(8)
O10-Co2-O11	84.55(10)	O1-Co2-O21	85.98(7)
O14-Co2-O11	90.90(10)	O9-Co2-O21	91.45(7)
O12-Co2-Co4	42.50(7)	O8-Co3-O11	86.10(7)
O9-Co2-Co4	133.89(8)	O8-Co3-O1	88.79(7)
O6-Co2-Co4	133.03(8)	O11-Co3-O1	174.79(7)
O10-Co2-Co4	91.53(8)	O8-Co3-O2	173.91(7)
O14-Co2-Co4	82.39(7)	O11-Co3-O2	92.39(7)
O11-Co2-Co4	43.87(7)	O1-Co3-O2	92.59(7)
O17-Co3-O4	88.69(11)	O8-Co3-O23	100.69(8)
O17-Co3-O13	93.10(11)	O11-Co3-O23	91.20(8)
O4-Co3-O13	177.87(11)	O1-Co3-O23	90.73(7)
O17-Co3-O10	176.29(11)	O2-Co3-O23	85.23(7)
O4-Co3-O10	89.76(10)	O8-Co3-O21	102.81(7)
O13-Co3-O10	88.39(10)	O11-Co3-O21	106.32(7)
O17-Co3-O16	92.70(11)	O1-Co3-O21	73.85(6)
O4-Co3-O16	91.05(11)	O2-Co3-O21	71.94(6)
O13-Co3-O16	90.01(10)	O23-Co3-O21	151.44(7)
O10-Co3-O16	90.70(10)	O2-Co4-O15	96.50(8)
O17-Co3-O11	104.31(10)	O2-Co4-O13	97.49(8)
O4-Co3-O11	105.18(9)	O15-Co4-O13	92.05(8)
O13-Co3-O11	73.27(9)	O2-Co4-O22	86.77(8)
O10-Co3-O11	72.86(9)	O15-Co4-O22	91.31(8)
O16-Co3-O11	156.52(10)	O13-Co4-O22	174.24(8)
O13-Co4-O21	96.44(11)	O2-Co4-O21	84.47(7)
O13-Co4-O12	86.07(11)	O15-Co4-O21	174.75(7)
O21-Co4-O12	174.90(11)	O13-Co4-O21	92.93(7)
O13-Co4-O19	97.42(11)	O22-Co4-O21	83.58(7)
O21-Co4-O19	91.40(11)	O2-Co4-O10	175.50(7)
O12-Co4-O19	92.67(11)	O15-Co4-O10	86.77(8)
O13-Co4-O15	174.19(11)	O13-Co4-O10	85.45(8)
O21-Co4-O15	86.88(11)	O22-Co4-O10	90.08(8)
O12-Co4-O15	90.26(10)	O21-Co4-O10	91.99(7)
O19-Co4-O15	87.25(10)	O16-Co5-O14	88.86(11)
O13-Co4-O11	84.78(10)	O16-Co5-O2	90.77(8)
O21-Co4-O11	91.38(10)	O14-Co5-O2	91.74(8)
O12-Co4-O11	84.42(10)	O16-Co5-O17	92.73(10)
O19-Co4-O11	176.24(11)	O14-Co5-O17	173.50(8)
O15-Co4-O11	90.37(10)	O2-Co5-O17	81.94(7)
O18-Co5-O13	95.74(11)	O16-Co5-O24	88.77(10)
O18-Co5-O25	89.09(12)	O14-Co5-O24	93.96(10)
O13-Co5-O25	170.52(12)	O2-Co5-O24	174.27(9)
O18-Co5-O22	93.39(13)	O17-Co5-O24	92.38(9)
O13-Co5-O22	94.98(11)	O16-Co5-O12	177.95(10)
O25-Co5-O22	92.86(12)	O14-Co5-O12	91.24(10)
O18-Co5-O20	177.42(11)	O2-Co5-O12	91.27(8)
O13-Co5-O20	85.48(11)	O17-Co5-O12	87.39(9)
O25-Co5-O20	89.38(12)	O24-Co5-O12	89.18(10)
O22-Co5-O20	88.77(12)		
O18-Co5-O23	86.10(11)		
O13-Co5-O23	85.40(10)		
O25-Co5-O23	86.80(11)		
O22-Co5-O23	179.39(11)		
O20-Co5-O23	91.74(11)		
Co2-O10-Co1	115.50(12)		
Co2-O10-Co3	104.06(12)		
Co1-O10-Co3	124.37(12)		
Co2-O11-Co4	92.66(10)		
Co2-O11-Co3	98.53(10)		
Co4-O11-Co3	97.39(9)		
Co2-O12-Co4	95.25(11)		
Co4-O13-Co5	118.53(13)		
Co4-O13-Co3	104.55(11)		
Co5-O13-Co3	120.99(12)		

Table 13. Bond lengths [Å] and angles [°] for **10**.

Co1−O1	2.0165(14)	Co3−O1	1.8665(13)
Co1−O13	2.0403(14)	Co3−O1	1.8845(13)
Co1−O7	2.0451(15)	Co3−O10	1.9189(14)
Co1−O4	2.0709(15)	Co3−O12	1.9223(14)
Co1−O2	2.1569(15)	Co3−O6	1.9283(14)
Co1−O6	2.3222(14)	Co3−O9	1.9311(14)
Co2−O1	1.9432(14)	Co2−O5	1.9796(14)
Co2−O5	1.9796(14)	Co2−O8	1.9805(14)
O1-Co1-O13	96.67(5)	O1-Co3-O1	83.80(6)
O1-Co1-O7	95.00(5)	O1-Co3-O10	97.62(6)
O13-Co1-O7	166.53(6)	O1-Co3-O10	88.87(6)
O1-Co1-O4	97.88(5)	O1-Co3-O12	97.17(6)
O13-Co1-O4	88.47(6)	O1-Co3-O12	174.32(6)
O7-Co1-O4	96.59(6)	O10-Co3-O12	85.46(6)
O1-Co1-O2	173.32(6)	O1-Co3-O6	85.42(6)
O13-Co1-O2	84.04(6)	O1-Co3-O6	96.84(6)
O7-Co1-O2	83.60(6)	O10-Co3-O6	173.81(6)
O4-Co1-O2	88.77(6)	O12-Co3-O6	88.82(6)
O1-Co1-O6	72.40(5)	O1-Co3-O9	173.51(6)
O13-Co1-O6	82.01(5)	O1-Co3-O9	94.74(6)
O7-Co1-O6	95.17(5)	O10-Co3-O9	88.66(6)
O4-Co1-O6	165.37(5)	O12-Co3-O9	84.90(6)
O2-Co1-O6	101.18(5)	O6-Co3-O9	88.48(6)
O1-Co2-O5	111.65(6)	Co3-O1-Co3	96.01(6)
O1-Co2-O8	104.77(6)	Co3-O1-Co2	119.42(7)
O5-Co2-O8	96.37(6)	Co3-O1-Co2	105.73(6)
O1-Co2-O11	103.73(6)	Co3-O1-Co1	103.12(6)
O5-Co2-O11	102.65(6)	Co3-O1-Co1	123.52(7)
O8-Co2-O11	136.63(6)	Co2-O1-Co1	109.48(6)

Table 14. Bond lengths [Å] and angles [°] for **11**.

Co1−O1	2.020(2)	Co4−O2	1.884(2)
Co1−O1C	2.034(2)	Co4−O1	1.884(2)
Co1−O1A	2.048(2)	Co4−O1I	1.924(2)
Co1−O1B	2.075(2)	Co4−O1G	1.932(2)
Co1−O1K	2.180(3)	Co4−O2F	1.935(2)
Co1−O1D	2.267(2)	Co4−O2C	1.937(2)
Co2−O1F	2.013(2)	Co5−O2	2.029(2)
Co2−O1	2.031(2)	Co5−O2D	2.054(3)
Co2−O1E	2.045(2)	Co5−O2I	2.058(3)
Co2−O2A	2.106(2)	Co5−O1J	2.079(2)
Co2−O1L	2.182(3)	Co5−O1M	2.166(3)
Co2−O1G	2.291(2)	Co5−O2C	2.254(2)
Co3−O1	1.878(2)	Co6−O2	2.003(2)
Co3−O2	1.881(2)	Co6−O2G	2.027(3)
Co3−O1H	1.938(2)	Co6−O2H	2.045(3)
Co3−O1D	1.942(2)	Co6−O2J	2.062(3)
Co3−O2E	1.947(2)	Co6−O1N	2.197(3)
Co3−O2B	1.961(2)	Co6−O2E	2.410(2)
O1-Co1-O1C	97.09(9)	O1-Co4-O2F	96.50(9)
O1-Co1-O1A	100.00(9)	O1I-Co4-O2F	83.49(10)
O1C-Co1-O1A	97.54(10)	O1G-Co4-O2F	88.78(10)
O1-Co1-O1B	97.13(9)	O2-Co4-O2C	86.16(10)
O1C-Co1-O1B	164.46(10)	O1-Co4-O2C	98.24(10)
O1A-Co1-O1B	86.12(9)	O1I-Co4-O2C	88.84(11)
O1-Co1-O1K	175.32(9)	O1G-Co4-O2C	174.22(10)
O1C-Co1-O1K	81.01(10)	O2F-Co4-O2C	86.48(10)
O1A-Co1-O1K	84.51(10)	O2-Co5-O2D	96.69(10)
O1B-Co1-O1K	84.33(10)	O2-Co5-O2I	96.05(10)
O1-Co1-O1D	74.13(9)	O2D-Co5-O2I	166.19(11)
O1C-Co1-O1D	95.15(9)	O2-Co5-O1J	99.90(10)
O1A-Co1-O1D	166.61(9)	O2D-Co5-O1J	94.63(11)
O1B-Co1-O1D	82.77(9)	O2I-Co5-O1J	88.38(10)
O1K-Co1-O1D	101.72(9)	O2-Co5-O1M	173.53(10)
O1F-Co2-O1	96.84(9)	O2D-Co5-O1M	82.26(12)
O1F-Co2-O1E	164.28(10)	O2I-Co5-O1M	84.48(12)
O1-Co2-O1E	97.01(9)	O1J-Co5-O1M	86.56(11)
O1F-Co2-O2A	88.89(10)	O2-Co5-O2C	74.88(8)
O1-Co2-O2A	97.48(9)	O2D-Co5-O2C	93.95(10)
O1E-Co2-O2A	96.64(9)	O2I-Co5-O2C	84.27(9)
O1F-Co2-O1L	84.70(10)	O1J-Co5-O2C	170.44(10)
O1-Co2-O1L	175.55(9)	O1M-Co5-O2C	98.78(10)
O1E-Co2-O1L	80.95(9)	O2-Co6-O2G	96.93(10)
O2A-Co2-O1L	86.71(9)	O2-Co6-O2H	97.64(10)
O1F-Co2-O1G	84.78(9)	O2G-Co6-O2H	159.60(12)
O1-Co2-O1G	73.45(9)	O2-Co6-O2J	100.78(10)
O1E-Co2-O1G	92.08(9)	O2G-Co6-O2J	102.77(11)
O2A-Co2-O1G	168.17(9)	O2H-Co6-O2J	88.44(10)
O1L-Co2-O1G	102.60(9)	O2-Co6-O1N	175.68(11)
O1-Co3-O2	83.88(9)	O2G-Co6-O1N	79.18(11)
O1-Co3-O1H	173.32(10)	O2H-Co6-O1N	85.69(12)
O2-Co3-O1H	96.77(9)	O2J-Co6-O1N	82.01(11)
O1-Co3-O1D	85.40(9)	O2-Co6-O2E	72.37(8)
O2-Co3-O1D	98.69(10)	O2G-Co6-O2E	90.79(9)
O1H-Co3-O1D	87.92(10)	O2H-Co6-O2E	80.13(9)
O1-Co3-O2E	99.35(9)	O2J-Co6-O2E	165.59(10)
O2-Co3-O2E	86.58(10)	O1N-Co6-O2E	105.64(10)
O1H-Co3-O2E	87.34(10)	Co3-O1-Co4	96.29(9)
O1D-Co3-O2E	173.30(10)	Co3-O1-Co1	101.66(10)
O1-Co3-O2B	95.68(9)	Co4-O1-Co1	120.68(11)
O2-Co3-O2B	172.66(10)	Co3-O1-Co2	120.19(10)
O1H-Co3-O2B	84.51(9)	Co4-O1-Co2	101.33(10)
O1D-Co3-O2B	88.57(10)	Co1-O1-Co2	116.13(10)
O2E-Co3-O2B	86.27(10)	Co3-O1-Co1′	121.5(2)
O2-Co4-O1	83.63(9)	Co3-O2-Co4	96.18(10)
O2-Co4-O1I	97.30(10)	Co3-O2-Co6	104.35(10)
O1-Co4-O1I	172.92(10)	Co4-O2-Co6	120.19(12)
O2-Co4-O1G	98.63(10)	Co3-O2-Co5	120.97(12)
O1-Co4-O1G	85.57(10)	Co4-O2-Co5	100.10(9)
O1I-Co4-O1G	87.35(10)	Co6-O2-Co5	114.63(10)

Table 15. Bond lengths [Å] and angles [°] for **12**.

Co1−O7	1.844(3)	Co3−O14	1.930(3)
Co1−O5	1.873(4)	Co4−O5	1.857(3)
Co1−O1	1.907(4)	Co4−O20	1.873(3)
Co1−O6	1.911(3)	Co4−O6	1.905(3)
Co1−O3	1.929(4)	Co4−O16	1.915(3)
Co1−O8	1.945(3)	Co4−O10	1.919(3)
Co2−O5	1.850(3)	Co4−O18	1.940(4)
Co2−O7	1.861(3)	Co5−O15	1.952(3)
Co2−O20	1.902(3)	Co5−O6	1.956(3)
Co2−O2	1.927(3)	Co5−O17	1.969(4)
Co2−O9	1.936(4)	Co5−O22	2.017(5)
Co2−O11	1.937(3)	Co5−O21	2.391(6)
Co3−O7	1.865(3)	Co6−O20	1.926(3)
Co3−O6	1.877(3)	Co6−O23	1.947(4)
Co3−O20	1.912(3)	Co6−O19	1.952(4)
Co3−O4	1.912(3)	Co6−O13	1.959(4)
Co3−O12	1.922(3)		
O7-Co1-O5	85.78(15)	O20-Co4-O6	82.89(14)
O7-Co1-O1	88.02(15)	O5-Co4-O16	91.11(15)
O5-Co1-O1	90.90(15)	O20-Co4-O16	177.18(14)
O7-Co1-O6	86.39(13)	O6-Co4-O16	97.42(15)
O5-Co1-O6	80.44(14)	O5-Co4-O10	91.65(15)
O1-Co1-O6	170.01(15)	O20-Co4-O10	90.11(14)
O7-Co1-O3	89.75(15)	O6-Co4-O10	170.14(15)
O5-Co1-O3	172.51(13)	O16-Co4-O10	89.23(15)
O1-Co1-O3	94.96(16)	O5-Co4-O18	177.46(15)
O6-Co1-O3	93.29(14)	O20-Co4-O18	95.25(14)
O7-Co1-O8	177.58(16)	O6-Co4-O18	97.06(15)
O5-Co1-O8	95.80(15)	O16-Co4-O18	87.50(15)
O1-Co1-O8	90.12(16)	O10-Co4-O18	90.47(15)
O6-Co1-O8	95.67(15)	O15-Co5-O6	101.33(13)
O3-Co1-O8	88.86(15)	O15-Co5-O17	122.66(18)
O5-Co2-O7	85.96(15)	O6-Co5-O17	101.85(15)
O5-Co2-O20	85.52(13)	O15-Co5-O22	130.56(19)
O7-Co2-O20	80.85(14)	O6-Co5-O22	100.87(18)
O5-Co2-O2	89.24(16)	O17-Co5-O22	94.8(2)
O7-Co2-O2	89.61(15)	O15-Co5-O21	90.94(16)
O20-Co2-O2	169.40(14)	O6-Co5-O21	158.53(19)
O5-Co2-O9	90.11(15)	O17-Co5-O21	85.8(2)
O7-Co2-O9	172.14(15)	O22-Co5-O21	58.2(2)
O20-Co2-O9	92.08(14)	O20-Co6-O23	129.97(16)
O2-Co2-O9	97.14(15)	O20-Co6-O19	102.36(14)
O5-Co2-O11	179.09(14)	O23-Co6-O19	100.99(17)
O7-Co2-O11	94.43(14)	O20-Co6-O13	103.75(14)
O20-Co2-O11	95.35(14)	O23-Co6-O13	103.71(16)
O2-Co2-O11	89.94(16)	O19-Co6-O13	117.26(15)
O9-Co2-O11	89.60(15)	Co2-O5-Co4	94.11(14)
O7-Co3-O6	86.81(14)	Co2-O5-Co1	93.17(16)
O7-Co3-O20	80.48(14)	Co4-O5-Co1	100.81(15)
O6-Co3-O20	82.60(14)	Co3-O6-Co4	97.03(14)
O7-Co3-O4	91.87(14)	Co3-O6-Co1	90.92(15)
O6-Co3-O4	90.18(14)	Co4-O6-Co1	97.74(14)
O20-Co3-O4	169.73(13)	Co3-O6-Co5	122.07(16)
O7-Co3-O12	90.97(14)	Co4-O6-Co5	113.81(18)
O6-Co3-O12	177.36(15)	Co1-O6-Co5	128.56(17)
O20-Co3-O12	98.44(14)	Co1-O7-Co2	93.77(15)
O4-Co3-O12	88.47(14)	Co1-O7-Co3	93.42(15)
O7-Co3-O14	177.30(14)	Co2-O7-Co3	100.90(16)
O6-Co3-O14	95.24(14)	Co4-O20-Co2	91.96(13)
O20-Co3-O14	98.01(14)	Co4-O20-Co3	96.95(14)
O4-Co3-O14	89.89(14)	Co2-O20-Co3	97.76(15)
O12-Co3-O14	87.03(14)	Co4-O20-Co6	122.66(17)
O5-Co4-O20	86.16(14)	Co2-O20-Co6	128.32(16)
O5-Co4-O6	81.00(14)	Co3-O20-Co6	112.61(15)

Table 16. Bond lengths [Å] and angles [°] for **13**.

Co7−O29	1.872(3)	Co10−O30	1.908(3)
Co7−O28	1.881(3)	Co10−O45	1.919(3)
Co7−O30	1.886(3)	Co10−O43	1.937(3)
Co7−O36	1.929(3)	Co10−O48	1.951(3)
Co7−O32	1.937(3)	Co11−O33	1.992(3)
Co7−O34	1.945(3)	Co11−O47	1.996(3)
Co8−O31	1.807(3)	Co11−O28	2.018(3)
Co8−O28	1.909(3)	Co11−O7	2.035(3)
Co8−O29	1.913(3)	Co11−N1	2.166(4)
Co8−O42	1.921(3)	Co12−O41	1.982(3)
Co8−O38	1.923(3)	Co12−O29	1.989(3)
Co8−O40	1.934(3)	Co12−O35	2.032(3)
Co9−O31	1.803(3)	Co12−O8	2.067(3)
Co9−O28	1.904(3)	Co12−O50	2.162(3)
Co9−O30	1.907(3)	Co13−O37	1.977(3)
Co9−O39	1.929(3)	Co13−O49	1.979(3)
Co9−O44	1.935(3)	Co13−O30	2.019(3)
Co9−O46	1.936(3)	Co13−O9	2.040(3)
Co10−O31	1.801(3)	Co13−N2	2.214(4)
Co10−O29	1.905(3)		
O29-Co7-O28	84.63(12)	O29-Co10-O48	97.83(12)
O29-Co7-O30	84.35(12)	O30-Co10-O48	100.13(12)
O28-Co7-O30	83.89(11)	O45-Co10-O48	91.35(12)
O29-Co7-O36	173.84(12)	O43-Co10-O48	88.17(13)
O28-Co7-O36	89.93(12)	O33-Co11-O47	148.19(14)
O30-Co7-O36	97.98(12)	O33-Co11-O28	96.42(12)
O29-Co7-O32	88.28(12)	O47-Co11-O28	95.84(12)
O28-Co7-O32	98.21(12)	O33-Co11-O7	98.28(13)
O30-Co7-O32	172.12(13)	O47-Co11-O7	110.22(14)
O36-Co7-O32	89.63(12)	O28-Co11-O7	93.13(12)
O29-Co7-O34	96.00(13)	O33-Co11-N1	83.66(15)
O28-Co7-O34	173.03(12)	O47-Co11-N1	82.00(15)
O30-Co7-O34	89.25(12)	O28-Co11-N1	175.69(14)
O36-Co7-O34	89.74(13)	O7-Co11-N1	91.12(15)
O32-Co7-O34	88.76(12)	O41-Co12-O29	99.05(12)
O31-Co8-O28	85.09(12)	O41-Co12-O35	149.51(13)
O31-Co8-O29	84.56(11)	O29-Co12-O35	98.04(11)
O28-Co8-O29	82.74(12)	O41-Co12-O8	111.40(14)
O31-Co8-O42	87.29(13)	O29-Co12-O8	91.13(12)
O28-Co8-O42	170.33(12)	O35-Co12-O8	93.27(13)
O29-Co8-O42	90.63(12)	O41-Co12-O50	79.54(13)
O31-Co8-O38	86.38(12)	O29-Co12-O50	175.31(14)
O28-Co8-O38	92.62(12)	O35-Co12-O50	85.18(13)
O29-Co8-O38	170.14(12)	O8-Co12-O50	85.26(14)
O42-Co8-O38	92.83(12)	O37-Co13-O49	147.12(14)
O31-Co8-O40	173.23(13)	O37-Co13-O30	97.30(12)
O28-Co8-O40	94.90(12)	O49-Co13-O30	95.39(12)
O29-Co8-O40	102.17(12)	O37-Co13-O9	98.74(15)
O42-Co8-O40	93.37(13)	O49-Co13-O9	110.33(15)
O38-Co8-O40	86.86(12)	O30-Co13-O9	94.59(12)
O31-Co9-O28	85.37(12)	O37-Co13-N2	82.61(15)
O31-Co9-O30	84.93(12)	O49-Co13-N2	82.78(15)
O28-Co9-O30	82.68(11)	O30-Co13-N2	176.18(14)
O31-Co9-O39	86.77(13)	O9-Co13-N2	89.19(15)
O28-Co9-O39	91.80(12)	Co7-O28-Co9	96.79(12)
O30-Co9-O39	170.37(13)	Co7-O28-Co8	96.10(13)
O31-Co9-O44	86.18(13)	Co9-O28-Co8	90.82(11)
O28-Co9-O44	170.21(13)	Co7-O28-Co11	110.41(13)
O30-Co9-O44	91.64(12)	Co9-O28-Co11	121.67(14)
O39-Co9-O44	92.67(12)	Co8-O28-Co11	133.38(14)
O31-Co9-O46	173.75(13)	Co7-O29-Co10	96.55(12)
O28-Co9-O46	100.82(13)	Co7-O29-Co8	96.26(13)
O30-Co9-O46	96.58(13)	Co10-O29-Co8	91.26(11)
O39-Co9-O46	92.19(13)	Co7-O29-Co12	108.66(13)
O44-Co9-O46	87.71(13)	Co10-O29-Co12	137.25(15)
O31-Co10-O29	84.95(12)	Co8-O29-Co12	118.58(13)
O31-Co10-O30	84.97(12)	Co7-O30-Co10	96.02(12)
O29-Co10-O30	82.85(12)	Co7-O30-Co9	96.50(12)
O31-Co10-O45	86.16(12)	Co10-O30-Co9	91.02(12)
O29-Co10-O45	170.37(12)	Co7-O30-Co13	111.69(13)

Table 16 (cont.)

O30-Co10-O45	92.71(12)	Co10-O30-Co13	121.63(14)
O31-Co10-O43	86.99(13)	Co9-O30-Co13	132.29(15)
O29-Co10-O43	90.20(12)	Co10-O31-Co9	98.05(13)
O30-Co10-O43	169.79(12)	Co10-O31-Co8	98.28(13)
O45-Co10-O43	93.02(13)	Co9-O31-Co8	97.53(13)
O31-Co10-O48	174.44(13)		

Table 17. Bond lengths [Å] and angles [°] for **14**.

Co1−O3	1.854(3)	Co3−O20	1.919(3)
Co1−O4	1.874(3)	Co3−O18	1.920(3)
Co1−O1	1.891(3)	Co4−O4	1.847(3)
Co1−O5	1.906(3)	Co4−O3	1.875(3)
Co1−O12	1.929(3)	Co4−O2	1.899(3)
Co1−O10	1.940(3)	Co4−O17	1.913(3)
Co2−O3	1.867(3)	Co4−O13	1.917(3)
Co2−O1	1.871(3)	Co4−O6	1.926(3)
Co2−O11	1.910(3)	Co5−O15	1.940(3)
Co2−O2	1.915(3)	Co5−O1	1.940(3)
Co2−O22	1.916(3)	Co5−O24	1.942(3)
Co2−O14	1.927(3)	Co5−O19	1.949(3)
Co3−O4	1.849(3)	Co6−O2	1.932(3)
Co3−O2	1.871(3)	Co6−O26	1.945(3)
Co3−O16	1.908(3)	Co6−O21	1.952(3)
Co3−O1	1.911(3)	Co6−O23	1.955(3)
O3-Co1-O4	86.30(13)	O4-Co4-O3	86.49(13)
O3-Co1-O1	85.69(13)	O4-Co4-O2	85.92(12)
O4-Co1-O1	81.20(12)	O3-Co4-O2	80.56(13)
O3-Co1-O5	178.13(15)	O4-Co4-O17	89.54(13)
O4-Co1-O5	94.78(14)	O3-Co4-O17	172.28(13)
O1-Co1-O5	95.98(14)	O2-Co4-O17	92.57(13)
O3-Co1-O12	89.61(16)	O4-Co4-O13	87.36(14)
O4-Co1-O12	89.41(14)	O3-Co4-O13	92.48(15)
O1-Co1-O12	169.74(15)	O2-Co4-O13	170.60(15)
O5-Co1-O12	88.88(16)	O17-Co4-O13	93.95(15)
O3-Co1-O10	89.30(15)	O4-Co4-O6	177.25(14)
O4-Co1-O10	172.13(13)	O3-Co4-O6	93.49(15)
O1-Co1-O10	91.98(13)	O2-Co4-O6	96.79(13)
O5-Co1-O10	89.81(15)	O17-Co4-O6	90.80(14)
O12-Co1-O10	97.08(15)	O13-Co4-O6	89.89(15)
O3-Co2-O1	85.88(13)	O15-Co5-O1	101.09(12)
O3-Co2-O11	91.02(14)	O15-Co5-O24	101.53(13)
O1-Co2-O11	89.97(14)	O1-Co5-O24	125.56(15)
O3-Co2-O2	80.35(13)	O15-Co5-O19	121.78(14)
O1-Co2-O2	82.89(12)	O1-Co5-O19	103.43(12)
O11-Co2-O2	169.14(13)	O24-Co5-O19	105.28(15)
O3-Co2-O22	90.99(14)	O2-Co6-O26	128.27(14)
O1-Co2-O22	176.82(14)	O2-Co6-O21	101.91(12)
O11-Co2-O22	89.54(15)	O26-Co6-O21	102.37(14)
O2-Co2-O22	97.15(13)	O2-Co6-O23	103.19(14)
O3-Co2-O14	177.72(14)	O26-Co6-O23	104.29(15)
O1-Co2-O14	95.65(12)	O21-Co6-O23	118.18(14)
O11-Co2-O14	90.67(13)	Co2-O1-Co1	92.50(13)
O2-Co2-O14	98.14(12)	Co2-O1-Co3	96.77(13)
O22-Co2-O14	87.49(13)	Co1-O1-Co3	97.34(12)
O4-Co3-O2	86.68(12)	Co2-O1-Co5	123.19(14)
O4-Co3-O16	90.95(13)	Co1-O1-Co5	128.20(15)
O2-Co3-O16	89.91(12)	Co3-O1-Co5	112.15(14)
O4-Co3-O1	81.32(12)	Co3-O2-Co4	91.48(12)
O2-Co3-O1	82.99(12)	Co3-O2-Co2	96.67(13)
O16-Co3-O1	169.76(13)	Co4-O2-Co2	98.23(13)
O4-Co3-O20	176.83(12)	Co3-O2-Co6	122.06(14)
O2-Co3-O20	95.54(12)	Co4-O2-Co6	128.60(15)
O16-Co3-O20	91.32(12)	Co2-O2-Co6	113.16(14)
O1-Co3-O20	96.68(12)	Co1-O3-Co2	93.87(14)
O4-Co3-O18	90.35(13)	Co1-O3-Co4	92.82(14)
O2-Co3-O18	176.42(12)	Co2-O3-Co4	100.84(15)
O16-Co3-O18	88.14(12)	Co4-O4-Co3	93.88(13)
O1-Co3-O18	98.54(12)	Co4-O4-Co1	93.04(13)
O20-Co3-O18	87.51(12)	Co3-O4-Co1	100.14(13)

Table 18. Bond lengths [Å] and angles [°] for **15**.

Co1−O1	1.866(3)	Co4−O15	2.103(3)
Co1−O2	1.887(3)	Co4−N1	2.123(4)
Co1−O5	1.900(3)	Co4−O3	2.256(3)
Co1−O6	1.905(3)	Co5−O21a	2.004(3)
Co1−O4	1.919(3)	Co5−O17	2.028(3)
Co1−O3	1.926(3)	Co5−O8	2.055(3)
Co2−O1	1.875(3)	Co5−O19	2.057(3)
Co2−O2	1.895(3)	Co5−O2	2.155(3)
Co2−O9	1.918(3)	Co5−O5	2.357(3)
Co2−O7	1.918(3)	Co6−O21	1.998(3)
Co2−O8	1.922(3)	Co6−O12	2.027(3)
Co2−O11	1.959(3)	Co6−O16a	2.035(3)
Co3−O1	1.867(3)	Co6−O22	2.121(3)
Co3−O12	1.901(3)	Co6−O4a	2.141(3)
Co3−O8	1.906(3)	Co6−O5a	2.285(3)
Co3−O5a	1.906(3)	Co7−O21	2.034(3)
Co3−O5	1.930(3)	Co7−O18a	2.081(3)
Co3−O3a	1.938(3)	Co7−O23	2.097(3)
Co4−O13	1.982(3)	Co7−O27	2.098(3)
Co4−O12a	2.090(3)	Co7−O20a	2.119(3)
Co4−O4	2.092(3)	Co7−O25	2.168(3)
O1-Co1-O2	85.87(12)	O8-Co5-O2	73.57(11)
O1-Co1-O5	84.83(12)	O19-Co5-O2	162.38(11)
O2-Co1-O5	87.81(12)	O21a-Co5-O5	85.44(10)
O1-Co1-O6	90.49(12)	O17-Co5-O5	160.81(11)
O2-Co1-O6	90.50(12)	O8-Co5-O5	77.31(10)
O5-Co1-O6	175.12(12)	O19-Co5-O5	96.38(10)
O1-Co1-O4	173.48(12)	O2-Co5-O5	71.02(10)
O2-Co1-O4	92.87(12)	O21-Co6-O12	165.63(11)
O5-Co1-O4	88.73(12)	O21-Co6-O16a	97.68(12)
O6-Co1-O4	95.92(12)	O12-Co6-O16a	96.07(11)
O1-Co1-O3	96.85(12)	O21-Co6-O22	94.13(11)
O2-Co1-O3	171.99(12)	O12-Co6-O22	87.79(11)
O5-Co1-O3	84.93(12)	O16a-Co6-O22	99.18(12)
O6-Co1-O3	97.00(12)	O21-Co6-O4a	93.09(11)
O4-Co1-O3	83.58(12)	O12-Co6-O4a	81.59(11)
O1-Co2-O2	85.38(12)	O16a-Co6-O4a	94.74(11)
O1-Co2-O9	88.31(12)	O22-Co6-O4a	163.31(11)
O2-Co2-O9	172.61(13)	O21-Co6-O5a	87.53(11)
O1-Co2-O7	90.96(12)	O12-Co6-O5a	78.18(10)
O2-Co2-O7	90.13(12)	O16a-Co6-O5a	168.01(11)
O9-Co2-O7	93.82(13)	O22-Co6-O5a	91.17(11)
O1-Co2-O8	83.55(12)	O4a-Co6-O5a	74.12(10)
O2-Co2-O8	82.71(12)	O21-Co7-O18a	96.88(11)
O9-Co2-O8	92.77(12)	O21-Co7-O23	177.75(12)
O7-Co2-O8	171.28(12)	O18a-Co7-O23	85.34(12)
O1-Co2-O11	172.87(13)	O21-Co7-O27	90.96(11)
O2-Co2-O11	88.22(13)	O18a-Co7-O27	172.15(12)
O9-Co2-O11	97.85(13)	O23-Co7-O27	86.82(12)
O7-Co2-O11	92.20(13)	O21-Co7-O20a	91.83(11)
O8-Co2-O11	92.54(13)	O18a-Co7-O20a	91.30(12)
O1-Co3-O12	93.86(12)	O23-Co7-O20a	88.47(12)
O1-Co3-O8	84.17(12)	O27-Co7-O20a	88.11(12)
O12-Co3-O8	91.14(12)	O21-Co7-O25	90.57(11)
O1-Co3-O5a	94.63(12)	O18a-Co7-O25	87.12(13)
O12-Co3-O5a	91.45(11)	O23-Co7-O25	89.18(12)
O8-Co3-O5a	177.22(12)	O27-Co7-O25	93.16(13)
O1-Co3-O5	83.94(12)	O20a-Co7-O25	177.26(11)
O12-Co3-O5	175.74(11)	Co1-O1-Co3	97.22(12)
O8-Co3-O5	92.27(12)	Co1-O1-Co2	93.94(12)
O5-Co3-O5a	85.10(12)	Co3-O1-Co2	97.48(12)
O1-Co3-O3a	178.34(12)	Co1-O2-Co2	92.62(13)
O12-Co3-O3a	84.80(11)	Co1-O2-Co5	104.24(13)
O8-Co3-O3a	96.82(12)	Co2-O2-Co5	99.71(12)
O5a-Co3-O3a	84.43(11)	Co1-O3-Co3a	94.28(12)
O5-Co3-O3a	97.33(12)	Co1-O3-Co4	98.81(12)
O13-Co4-O12a	99.51(12)	Co3a-O3-Co4	97.39(11)
O13-Co4-O4	177.84(13)	Co1-O4-Co4	104.96(12)
O12a-Co4-O4	81.32(11)	Co1-O4-Co6a	100.60(12)
O13-Co4-O15	96.02(13)	Co4-O4-Co6a	92.50(11)
O12a-Co4-O15	93.37(11)	Co1-O5-Co3a	96.16(12)
O4-Co4-O15	85.90(11)	Co1-O5-Co3	93.98(12)
O13-Co4-N1	84.25(14)	Co3a-O5-Co3	94.90(12)
O12a-Co4-N1	168.42(13)	Co1-O5-Co6a	96.28(11)
O4-Co4-N1	94.55(12)	Co3a-O5-Co6a	90.30(11)
O15-Co4-N1	97.13(13)	Co3-O5-Co6a	167.94(14)
O13-Co4-O3	106.19(13)	Co1-O5-Co5	96.64(11)
O12a-Co4-O3	73.00(10)	Co3a-O5-Co5	166.54(14)
O4-Co4-O3	72.10(10)	Co3-O5-Co5	88.34(10)
O15-Co4-O3	155.43(11)	Co6a-O5-Co5	84.20(9)
N1-Co4-O3	95.44(12)	Co3-O8-Co2	94.60(12)
O21a-Co5-O17	100.33(12)	Co3-O8-Co5	98.52(12)
O21a-Co5-O8	160.26(11)	Co2-O8-Co5	102.39(13)
O17-Co5-O8	93.21(11)	Co3-O12-Co6	98.81(12)
O21a-Co5-O19	99.47(12)	Co3-O12-Co4a	104.49(12)
O17-Co5-O19	100.64(12)	Co6-O12-Co4a	95.95(11)
O8-Co5-O19	91.98(11)	Co6-O21-Co5a	102.13(13)
O21a-Co5-O2	91.91(11)	Co6-O21-Co7	127.31(14)
O17-Co5-O2	90.39(11)	Co5a-O21-Co7	109.63(13)

CCDC-206549–206562 contain the supplementary crystallographic data for the structures reported in this paper. The structure of **4** has been recollected at 120 K since this paper was originally submitted. The refinement is improved but does not alter conclusions reached above. This re-determination has the code CCDC 211456. All crystallographic data can be obtained free of charge via www.ccdc.cam.ac.uk/conts/retrieving.html (or from the Cambridge Crystallographic Data Centre, 12 Union Road, Cambridge CB2 1EZ, UK; fax: (+44) 1223-336033; or e-mail: deposit@ccdc.cam.ac.uk).

Physical measurements: FTIR spectra were collected on a Perkin–Elmer Spectrum RXI spectrometer. Electronic ionization mass spectrometry was performed with a Hewlet–Packard 5890 Series II gas chromatograph coupled to a Fisons Instruments VG TRIO spectrometer. 300 MHz ^{1}H NMR spectra were measured on a Varian Unity Inova 300 instrument. Elemental analysis was performed in house with a Carlo Erba Instruments CHNS-O EA-1108 elemental analyzer.

Acknowledgements

This work was supported in part by INTAS (Grant: 00-0172). We are also grateful to the Royal Society for support for an Ex-Agreement Visit (G.A.T.), and to the EPSRC(UK) for funding for diffractometers and a postdoctoral position (G.A.), and to the University of Manchester.

---

[1] a) A. S. Batsanov, G. A. Timko, Y. T. Struchkov, N. V. Gérbéléu, K. M. Indrichan, *Koord. Khim.* **1991**, *17*, 662–669; b) F. E. Mabbs, E. J. L. McInnes, M. Murrie, S. Parsons, G. M. Smith, C. C. Wilson, R. E. P. Winpenny, *Chem. Commun.* **1999**, 643–644.

[2] a) N. V. Gerbeleu, Yu. T. Struchkov, G. A. Timco, A. S. Batsanov, K. M. Indrichan, G. A. Popovich, *Dokl. Akad. Nauk. SSSR* **1990**, *313*, 1459–1462; b) J. van Slageren, R. Sessoli, D. Gatteschi, A. A. Smith, M. Helliwell, R. E. P. Winpenny, A. Cornia, A.-L. Barra, A. G. M. Jansen, G. A. Timco, E. Rentschler, *Chem. Eur. J.* **2002**, *8*, 277–285.

[3] a) C. Wilson, B. B. Iversen, J. Overgaard, F. K. Larsen, G. Wu, S. P. Palii, G. A. Timco, N. V. Gerbeleu, *J. Am. Chem. Soc.* **2000**, *122*, 11370–11379; b) A. S. Batsanov, Yu. T. Struchkov, G. A. Timco, *Koord. Khim.* **1988**, *14*, 266–270; b) A. S. Batsanov, G. A. Timco, Yu. T. Struchkov, N. V. Gerbeleu, O. S. Manole, *Koord. Khim.* **1991**, *17*, 922–926.

[4] a) C. Benelli, E. K. Brechin, S. J. Coles, A. Graham, S. G. Harris, S. Meier, A. Parkin, S. Parsons, A. M. Seddon, R. E. P. Winpenny, *Chem. Eur. J.* **2000**, *6*, 883–896; b) E. K. Brechin, A. Graham, A. Parkin, S. Parsons, A. M. Seddon, R. E. P. Winpenny, *J. Chem. Soc. Dalton Trans.* **2000**, 3242–3252.

[5] a) I. L. Eremenko, S. E. Nefedov, A. A. Sidorov, M. A. Golubnichaya, P. V. Danilov, V. N. Ikorskii, Yu. G. Shvedenkov, V. M. Novotortsev, I. I. Moiseev, *Inorg. Chem.* **1999**, *38*, 3764 – 3773; b) A. A. Sidorov, M. O. Ponina, S. M. Deomidov, V. M. Novotortsev, A. Demonceau, S. E. Nefedov, I. L. Eremenko, I. I. Moiseev, *Chem. Commun.* **2000**, 1383 – 1384; c) M. A. Golubnichaya, A. A. Sidorov, I. G. Fomina, M. O. Ponina, S. M. Deomidov, S. E. Nefedov, I. L. Eremenko, I. I. Moiseev, *Russ. Chem. Bull.* **1999**, *48*, 1751 – 1756; d) M. A. Golubnichaya, A. A. Sidorov, I. G. Fomina, L. T. Eremenko, S. E. Nefedov, I. L. Eremenko, I. I. Moiseev, *Zh. Neorg. Khim.* **1999**, *44*, 1479 – 1484.

[6] Harris notation describes the binding mode as $[X.Y_1Y_2Y_3\ldots Y_n]$, in which X is the overall number of metals bound by the whole ligand, and each value of Y refers to the number of metal atoms attached to the different donor atoms. Therefore for both acetate and pivalate, there will be two values for Y. The ordering of Y is listed by the Cahn – Ingold – Prelog priority rules, hence O before N. See: R. A. Coxall, S. G. Harris, D. K. Henderson, S. Parsons, P. A. Tasker, R. E. P. Winpenny, *J. Chem. Soc. Dalton Trans.* **2000**, 2349 – 2356.

[7] a) I. D. Brown, *Acta Crystallogr. Sect. B* **1985**, *41*, 244 – 247; b) F. H. Allen, O. Kennard, *Chem. Des. Autom. News* **1993**, *8*, 31 – 37.

[8] A. A. Pasinschii, T. Ch. Indrisov, V. M. Novotortev, V. T. Kalinnicov, *Koord. Khim*. **1978**, *1*, 1057 – 1061.

[9] T. Sh. Gefeisman, A. A. Dvorkin, G. A. Timko, Yu. A. Simonov, N. V. Gerbeleu, G. A. Popovich. *Izv. Akad. Nauk Mold. SSR. Ser. Fiz.-Tekh. Mat. Nauk.* **1985**, 22 – 25.

[10] J. K. Beattie, T. W. Hambley, J. A. Kleptko, A. F. Masters, P. Turner, *Polyhedron* **1996**, *15*, 2141 – 2150.

[11] I. Bertini, C. Luchinat, *NMR of Paramagnetic Molecules in Biological Systems*, Benjamin/Cummings, Menlo Park, CA, **1986**.

[12] K. Dimitrou, J.-S. Sun, K. Folting, G. Christou, *Inorg. Chem.* **1995**, *34*, 4160 – 4166.

[13] V. A. Grillo, Z. Sun, K. Folting, D. N. Hendrickson, G. Christou, *Chem. Commun.* **1996**, 2233 – 2234.

[14] J. K. Beattie, T. W. Hambley, J. A. Kleptko, A. F. Masters, P. Turner, *Polyhedron*, **1997**, *16*, 2106 – 2112.

[15] S. Manole, A. S. Batsanov, Yu. T. Struchkov, G. A. Timco, L. D. Singerean, N. V. Gérbéléu, *Koord. Khim.* **1994**, *20*, 231 – 237.

[16] E. K. Brechin, W. Clegg, M. Murrie, S. Parsons, S. J. Teat, R. E. P. Winpenny, *J. Am. Chem. Soc.* **1998**, *120*, 7365 – 7366.

[17] S. Parsons, A. A. Smith, R. E. P. Winpenny, *Chem. Commun.* **2000**, 579 – 580.

[18] J. Cosier, A. M. Glazer, *J. Appl. Crystallogr.* **1986**, *19*, 105 – 107.

[19] SHELX-PC Package, Bruker Analytical X-ray Systems, Madison, WI, **1998**.

[20] P. T. Beurskens, G. Beurskens, W. P. Bosman, R. de Gelder, S. Garcia-Granda, R. O. Gould, R. Israel, J. M. M. Smits, DIRDIF-96 Program System, Crystallography Laboratory, University of Nijmegen **1996**.

[21] A. Parkin, S. Parsons, G. A. Timco, R. E. P. Winpenny, unpublished results.

Received: March 21, 2003 [F4993]